

Supplementary material S3.2

Contents of this file:

Section S3.2.1: Reference list for the compiled plant macrofossil records

Section S3.2.2: Figures S3.9–S3.84 – Age depth models for each core record

(Supplementary datasets S3.1 and S3.2 are uploaded separately)

Section S3.2.1: Reference list for the compiled plant macrofossil records

- Andersson, R.A., Kuhry, P., Meyers, P., Zebühr, Y., Crill, P. and Mörth, M. 2011. Impacts of paleohydrological changes on n-alkane biomarker compositions of a Holocene peat sequence in the eastern European Russian Arctic. *Organic Geochemistry*. **42**(9), pp.1065-1075.
- Bauer, I.E. and Vitt, D.H. 2011. Peatland dynamics in a complex landscape: Development of a fen-bog complex in the Sporadic Discontinuous Permafrost zone of northern Alberta, Canada. *Boreas*. **40**(4), pp.714-726.
- Beaulieu-Audy, V., Garneau, M., Richard, P.J. and Asnong, H. 2009. Holocene palaeoecological reconstruction of three boreal peatlands in the La Grande Rivière region, Québec, Canada. *The Holocene*. **19**(3), pp.459-476.
- Bhiry, N. and Robert, É.C. 2006. Reconstruction of changes in vegetation and trophic conditions of a palsa in a permafrost peatland, subarctic Québec, Canada. *Écoscience*. **13**(1), pp.56-65.
- de Klerk, P., Donner, N., Karpov, N.S., Minke, M. and Joosten, H. 2011. Short-term dynamics of a low-centred ice-wedge polygon near Chokurdakh (NE Yakutia, NE Siberia) and climate change during the last ca 1250 years. *Quaternary Science Reviews*. **30**(21-22), pp.3013-3031.
- Ellis, C.J. and Rochefort, L. 2004. Century-scale development of polygon-patterned tundra wetland, Bylot Island (73 N, 80 W). *Ecology*. **85**(4), pp.963-978.
- Fritz, M., Wolter, J., Rudaya, N., Palagushkina, O., Nazarova, L., Obu, J., Rethemeyer, J., Lantuit, H. and Wetterich, S. 2016. Holocene ice-wedge polygon development in northern Yukon permafrost peatlands (Canada). *Quaternary Science Reviews*. **147**, pp.279-297.
- Galka, M., Swindles, G.T., Szal, M., Fulweber, R. and Feurdean, A. 2018. Response of plant communities to climate change during the late Holocene: Palaeoecological insights from peatlands in the Alaskan Arctic. *Ecological Indicators*. **85**, pp.525-536.
- Heffernan, L., Estop-Aragónés, C., Knorr, K.H., Talbot, J. and Olefeldt, D., 2020. Long-term impacts of permafrost thaw on carbon storage in peatlands: deep losses offset

by surficial accumulation. *Journal of Geophysical Research: Biogeosciences*. **125**(3), p.e2019JG005501.

Hunt, S., Yu, Z. and Jones, M. 2013. Lateglacial and Holocene climate, disturbance and permafrost peatland dynamics on the Seward Peninsula, western Alaska. *Quaternary Science Reviews*. **63**, pp.42-58.

Kettles, I.M., Robinson, S.D., Bastien, D.F., Garneau, M., Hall, G.E.M. 2003. PHYSICAL, GEOCHEMICAL, MACROFOSSIL AND GROUND PENETRATING RADAR INFORMATION ON FOURTEEN PERMAFROST-AFFECTED PEATLANDS IN THE MACKENZIE VALLEY, NORTHWEST TERRITORIES (No. Open File 4007). Geological Survey of Canada.

Kjellman, S.E., Axelsson, P.E., Etzelmüller, B., Westermann, S. and Sannel, A.B.K. 2018. Holocene development of subarctic permafrost peatlands in Finnmark, northern Norway. *The Holocene*. **28**(12), pp.1855-1869.

Klein, E.S., Yu, Z. and Booth, R.K. 2013. Recent increase in peatland carbon accumulation in a thermokarst lake basin in southwestern Alaska. *Palaeogeography, Palaeoclimatology, Palaeoecology*. **392**, pp.186-195.

Kuhry, P. 2008. Palsa and peat plateau development in the Hudson Bay Lowlands, Canada: timing, pathways and causes. *Boreas*. **37**(2), pp.316-327.

Langlais, K., Bhiry, N. and Lavoie, M. 2021. Holocene dynamics of an inland palsa peatland at Wiyâshâkimî Lake (Nunavik, Canada). *Écoscience*. **28**(3-4), pp.269-282.

Leppänen, J.J., Piilo, S., Li, Y., Zhang, H. and Väiliranta, M. 2019. Paleoecological assessment of cladoceran community dynamics in two subarctic peatlands. *Wetlands*. **39**(4), pp.831-839.

Loisel, J. and Garneau, M. 2010. Late Holocene paleoecohydrology and carbon accumulation estimates from two boreal peat bogs in eastern Canada: Potential and limits of multi-proxy archives. *Palaeogeography, Palaeoclimatology, Palaeoecology*. **291**(3-4), pp.493-533.

Magnan, G., van Bellen, S., Davies, L., Froese, D., Garneau, M., Mullan-Boudreau, G., Zacccone, C. and Shotyk, W. 2018. Impact of the Little Ice Age cooling and 20th century climate change on peatland vegetation dynamics in central and northern

Alberta using a multi-proxy approach and high-resolution peat chronologies. *Quaternary Science Reviews*. **185**, pp.230-243.

Manies, K.L., Jones, M.C., Waldrop, M.P., Leewis, M.C., Fuller, C., Cornman, R.S. and Hoefke, K. 2021. Influence of permafrost type and site history on losses of permafrost carbon after thaw. *Journal of Geophysical Research: Biogeosciences*. **126**(11), p.e2021JG006396.

Nakatsubo, T., Uchida, M., Sasaki, A., Kondo, M., Yoshitake, S. and Kanda, H. 2015. Carbon accumulation rate of peatland in the High Arctic, Svalbard: Implications for carbon sequestration. *Polar Science*. **9**(2), pp.267-275.

Oksanen, P., Kuhry, P. and Alekseeva, R. 2003. Holocene development and permafrost history of the Usinsk mire, northeast European Russia. *Géographie physique et Quaternaire*. **57**(2-3), pp.169-187.

Oksanen, P.O., Kuhry, P. and Alekseeva, R.N. 2001. Holocene development of the Rogovaya river peat plateau, European Russian Arctic. *The Holocene*. **11**(1), pp.25-40.

Ouzilleau Samson, D., Bhiry, N. and Lavoie, M. 2010. Late-Holocene palaeoecology of a polygonal peatland on the south shore of Hudson Strait, northern Québec, Canada. *The Holocene*. **20**(4), pp.525-536.

Piilo, S.R., Zhang, H., Garneau, M., Gallego-Sala, A., Amesbury, M.J. and Väiliranta, M.M. 2019. Recent peat and carbon accumulation following the Little Ice Age in northwestern Québec, Canada. *Environmental Research Letters*. **14**(7), p.075002.

Primeau, G. and Garneau, M. 2021. Carbon accumulation in peatlands along a boreal to subarctic transect in eastern Canada. *The Holocene*. **31**(5), pp.858-869.

Robitaille, M., Garneau, M., van Bellen, S. and Sanderson, N.K. 2021. Long-term and recent ecohydrological dynamics of patterned peatlands in north-central Quebec (Canada). *The Holocene*. **31**(5), pp.844-857.

Routh, J., Hugelius, G., Kuhry, P., Filley, T., Tillman, P.K., Becher, M. and Crill, P. 2014. Multi-proxy study of soil organic matter dynamics in permafrost peat deposits reveal vulnerability to climate change in the European Russian Arctic. *Chemical geology*. **368**, pp.104-117.

Sannel, A.B.K. and Kuhry, P. 2008. Long-term stability of permafrost in subarctic peat plateaus, west-central Canada. *The Holocene*. **18**(4), pp.589-601.

Sannel, A.B.K., Hempel, L., Kessler, A. and Preskienis, V. 2018. Holocene development and permafrost history in sub-arctic peatlands in Tavvavuoma, northern Sweden. *Boreas*. **47**(2), pp.454-468.

Sim, T.G., Swindles, G.T., Morris, P.J., Baird, A.J., Cooper, C.L., Gallego-Sala, A.V., Charman, D.J., Roland, T.P., Borken, W., Mullan, D.J. and Aquino-Lopez, M.A. 2021. Divergent responses of permafrost peatlands to recent climate change. *Environmental Research Letters*. **16**(3), p.034001.

Sim, T.G., Swindles, G.T., Morris, P.J., Gałka, M., Mullan, D. and Galloway, J.M. 2019. Pathways for ecological change in Canadian High Arctic wetlands under rapid twentieth century warming. *Geophysical Research Letters*. **46**(9), pp.4726-4737.

Teltewskoi, A., Beermann, F., Beil, I., Bobrov, A., De Klerk, P., Lorenz, S., Lüder, A., Michaelis, D. and Joosten, H. 2016. 4000 years of changing wetness in a permafrost polygon peatland (Kytalyk, NE Siberia): A comparative high-resolution multi-proxy study. *Permafrost and Periglacial Processes*. **27**(1), pp.76-95.

Tremblay, S., Bhiry, N. and Lavoie, M. 2014. Long-term dynamics of a palsa in the sporadic permafrost zone of northwestern Quebec (Canada). *Canadian Journal of Earth Sciences*. **51**(5), pp.500-509.

Väliranta, M., Kaakinen, A. and Kuhry, P. 2003. Holocene climate and landscape evolution east of the Pechora Delta, East-European Russian Arctic. *Quaternary Research*. **59**(3), pp.335-344.

Väliranta, M., Marushchak, M.E., Tuovinen, J.P., Lohila, A., Biasi, C., Voigt, C., Zhang, H., Piilo, S., Virtanen, T., Räsänen, A. and Kaverin, D. 2021. Warming climate forcing impact from a sub-arctic peatland as a result of late Holocene permafrost aggradation and initiation of bare peat surfaces. *Quaternary Science Reviews*. **264**, p.107022.

Van Bellen, S., Garneau, M. and Booth, R.K. 2011. Holocene carbon accumulation rates from three ombrotrophic peatlands in boreal Quebec, Canada: impact of climate-driven ecohydrological change. *The Holocene*. **21**(8), pp.1217-1231.

Van Bellen, S., Garneau, M., Ali, A.A., Lamarre, A., Robert, E.C., Magnan, G., Asnong, H. and Pratte, S. 2013. Poor fen succession over ombrotrophic peat related to late Holocene increased surface wetness in subarctic Quebec, Canada. *Journal of Quaternary Science*. **28**(8), pp.748-760.

Vardy, S.R., Warner, B.G. and Aravena, R. 1997. Holocene Climate Effects on the Development of a Peatland on the Tuktoyaktuk Peninsula, Northwest Territories¹. *Quaternary Research*. **47**(1), pp.90-104.

Vardy, S.R., Warner, B.G. and Aravena, R. 1998. Holocene climate and the development of a subarctic peatland near Inuvik, Northwest Territories, Canada. *Climatic Change*. **40**(2), pp.285-313.

Vardy, S.R., Warner, B.G. and Asada, T. 2005. Holocene environmental change in two polygonal peatlands, south-central Nunavut, Canada. *Boreas*. **34**(3), pp.324-334.

Zhang, H., Amesbury, M.J., Piilo, S.R., Garneau, M., Gallego-Sala, A. and Väliranta, M.M. 2020. Recent changes in peatland testate amoeba functional traits and hydrology within a replicated site network in northwestern Québec, Canada. *Frontiers in Ecology and Evolution*. **8**, p.228.

Zhang, H., Piilo, S.R., Amesbury, M.J., Charman, D.J., Gallego-Sala, A.V. and Väliranta, M.M. 2018. The role of climate change in regulating Arctic permafrost peatland hydrological and vegetation change over the last millennium. *Quaternary Science Reviews*. **182**, pp.121-130.

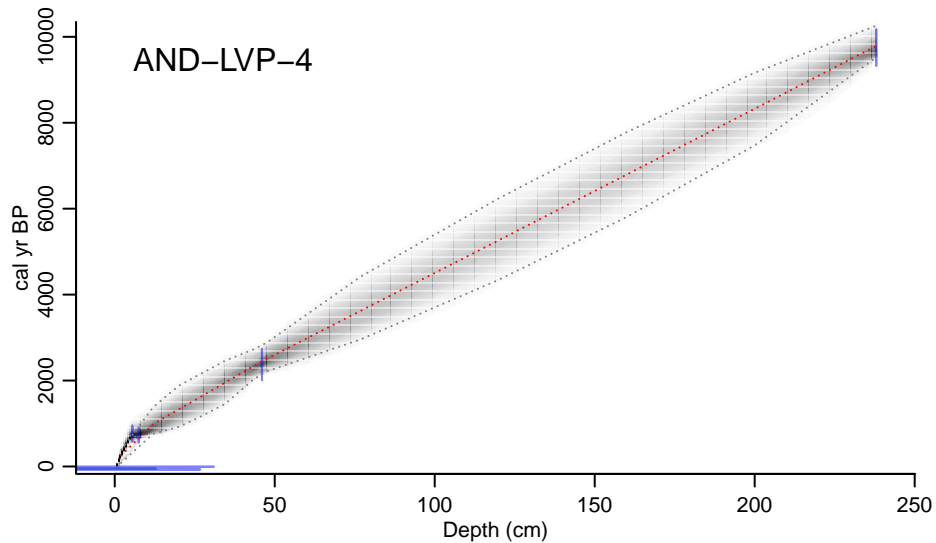
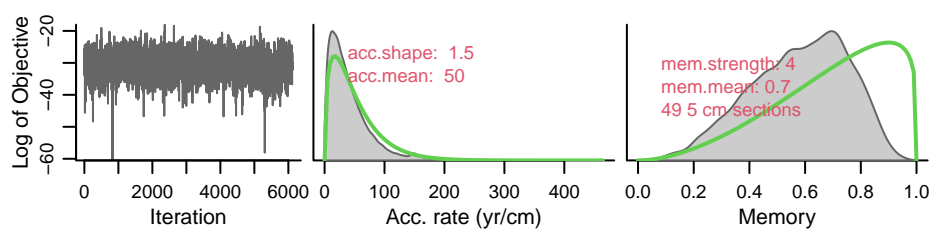
Section S3.2.2: Figures S3.9–S3.84 – Age depth models for each core record

The following age-depth model figures were generated using rBacon (v.2.5.7) (Blaauw and Christen, 2011), rplum (v.0.2.2) (Aquino-López et al., 2018), or clam (v.2.4.0) (Blaauw, 2010). For details on the modelling software used for each record, please see supplementary datasets S3.1 and S3.2.

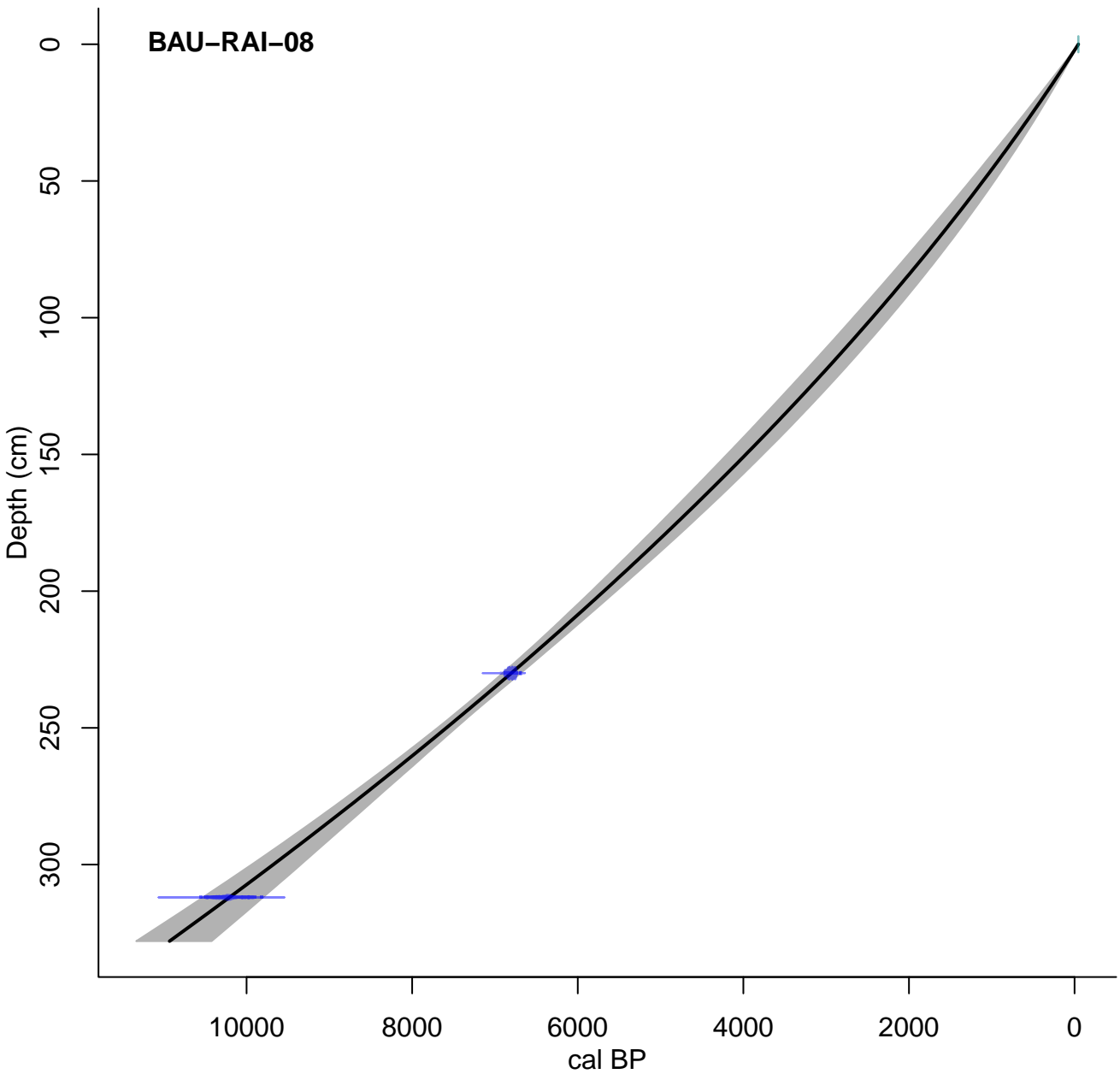
For Bacon age-depth model figures: top panels show the distribution of Markov Chain Monte Carlo (MCMC) iterations (left plot), the prior (green line) and posterior (grey shading) distributions for the accumulation rate (yr cm^{-1}) (centre plot) and memory (right plot). Prior settings for the accumulation rate and memory are reported in red text. The lower panel shows calibrated ^{14}C dates (blue), surface ages and calibrated ^{210}Pb dates (green), and the age-depth model (grey dashed lines indicated 95 % confidence interval; red dashed line indicates the mean age for each depth). Plum age-depth model figures show the same information with additions: plots indicating the prior (green line) and posterior (grey shading) distributions for ^{210}Pb influx (second from right) and the supported levels of ^{210}Pb for each depth (top right); and blue bars demonstrating the ^{210}Pb profile (overlain on the age-depth model). For clam models, plots show: calibrated ^{14}C dates (blue), surface ages (green), dates omitted from age-depth modelling (red), the age-depth model (black line), and 95 % confidence intervals (grey shading).

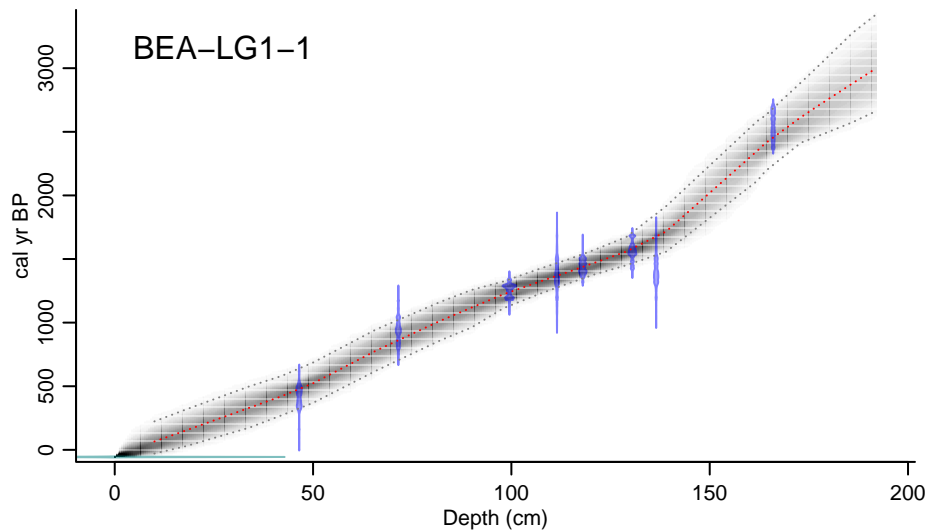
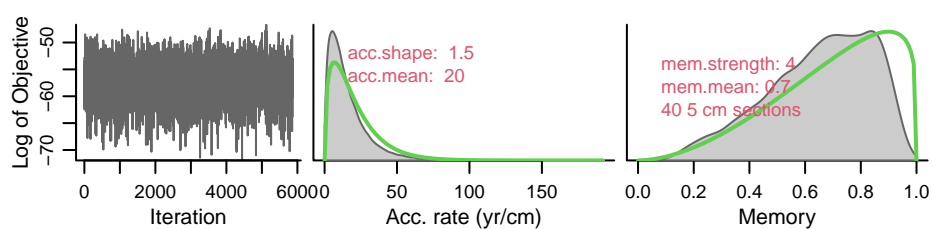
References:

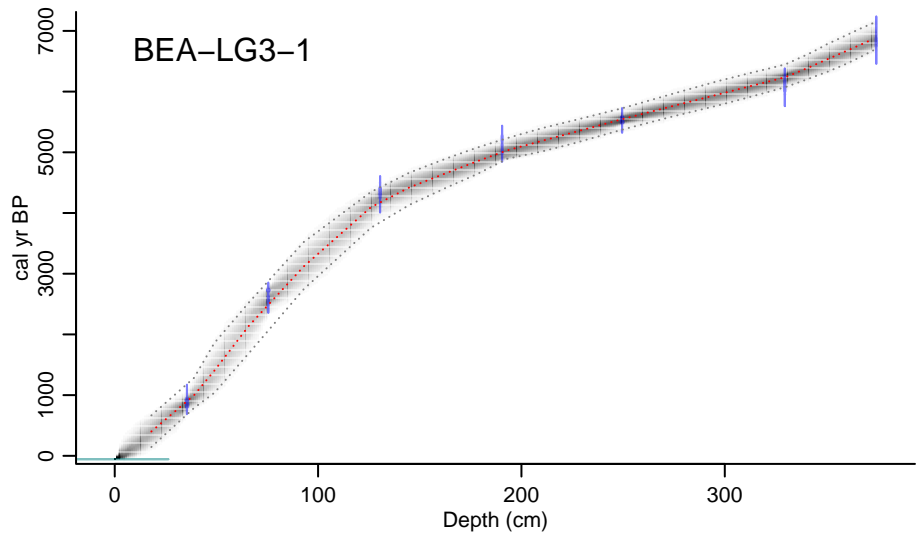
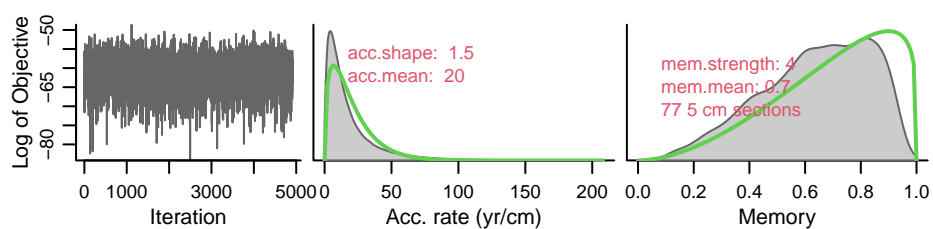
- Aquino-López, M.A., Blaauw, M., Christen, J.A. and Sanderson, N.K. 2018. Bayesian Analysis of ^{210}Pb Dating. *Journal of Agricultural, Biological and Environmental Statistics*. **23**(3), pp.317–333.
- Blaauw, M. 2010. Methods and code for ‘classical’ age-modelling of radiocarbon sequences. *Quaternary Geochronology*. **5**(5), pp.512–518.
- Blaauw, M. and Christen, J.A. 2011. Flexible paleoclimate age-depth models using an autoregressive gamma process. *Bayesian Analysis*. **6**(3), pp.457–474.

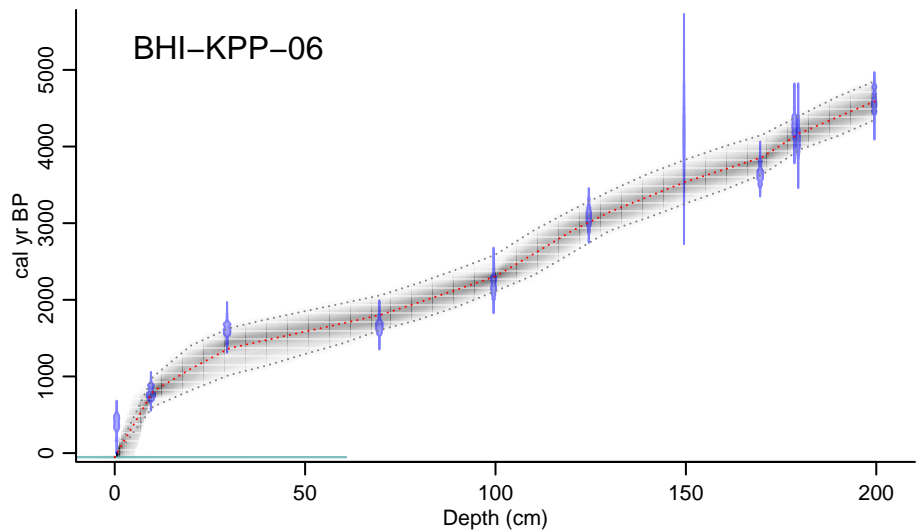
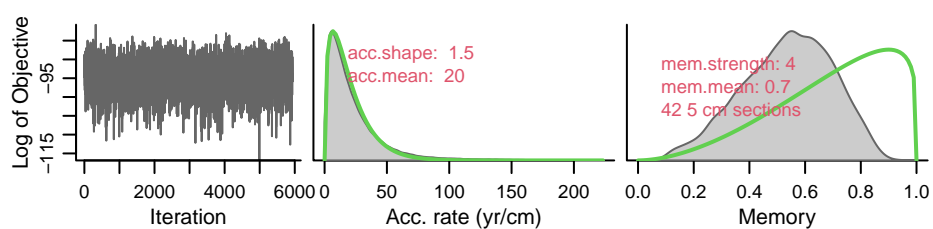


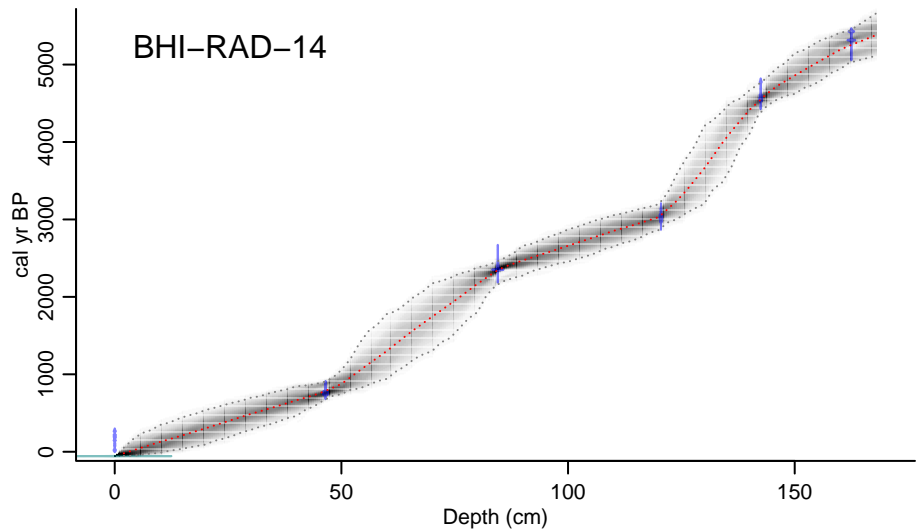
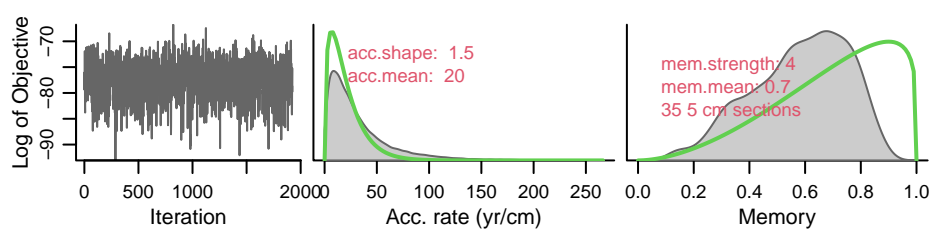
BAU-RAI-08



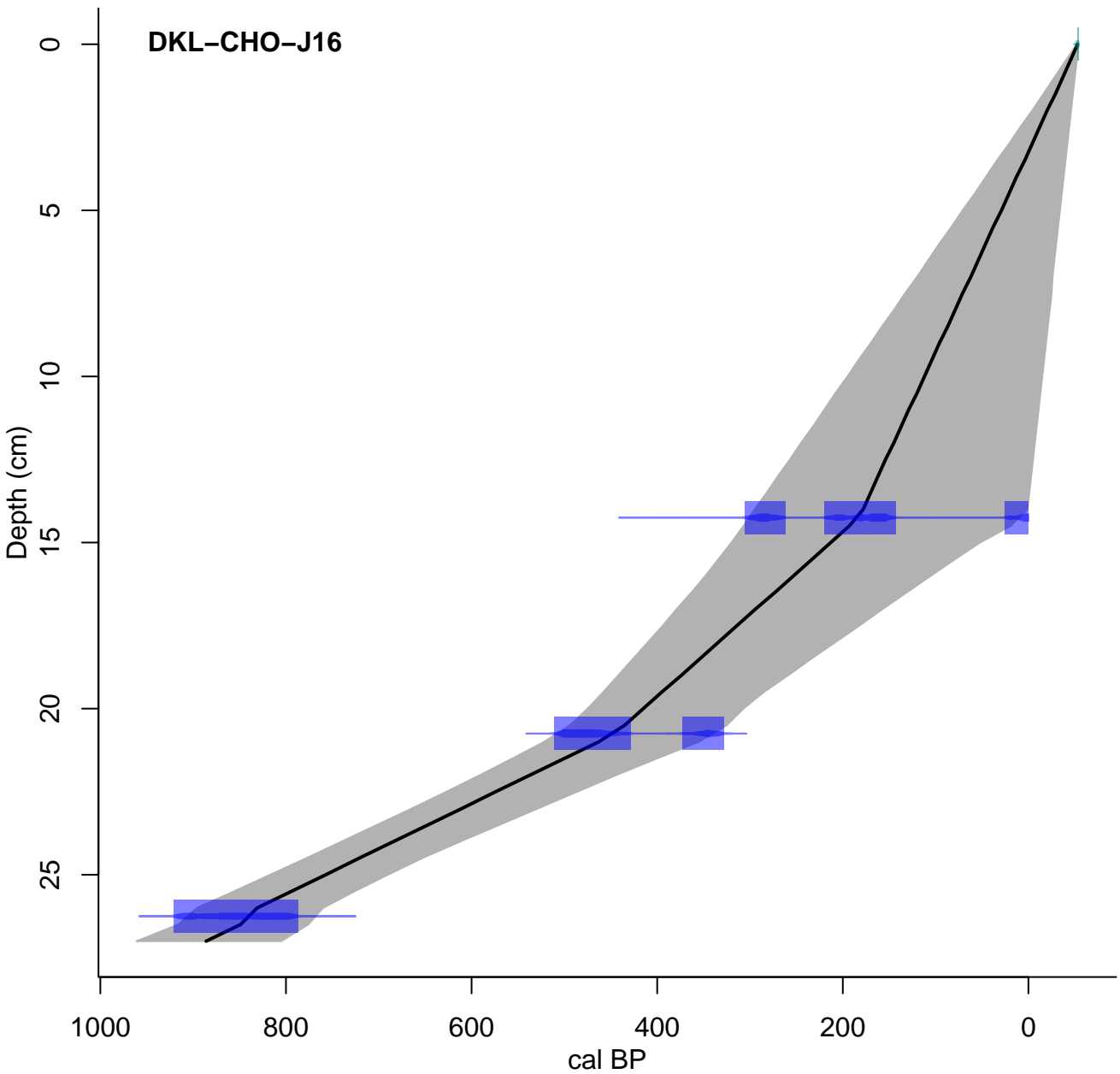


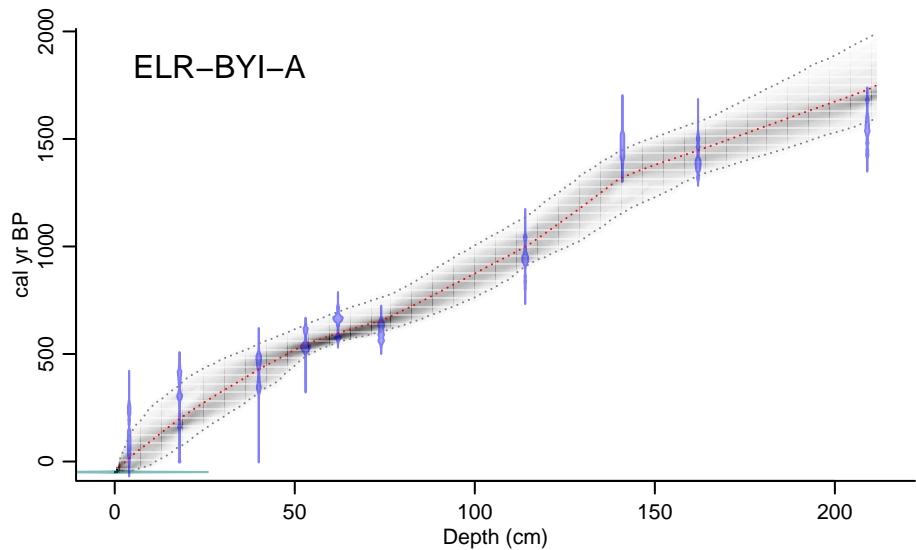
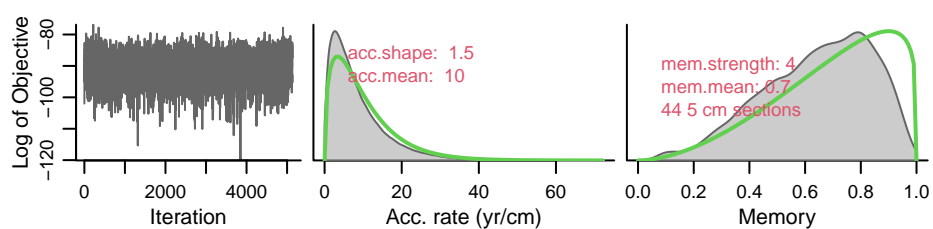


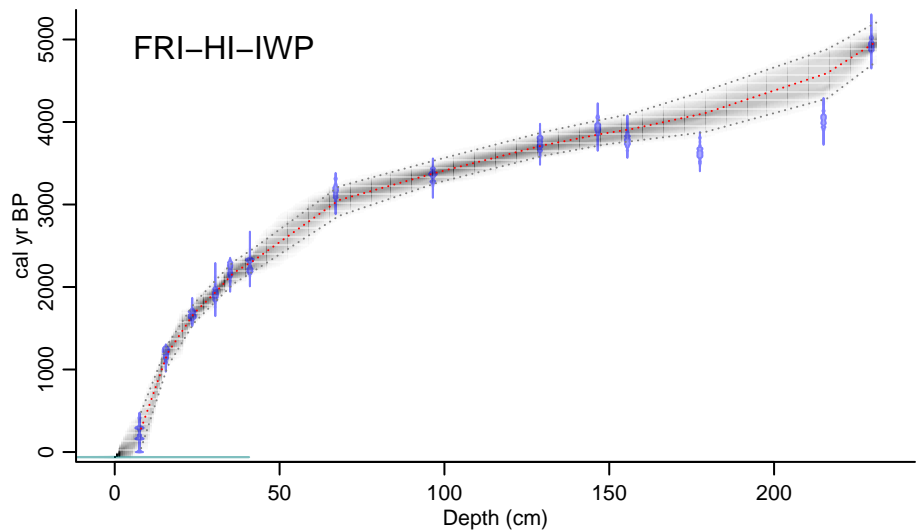
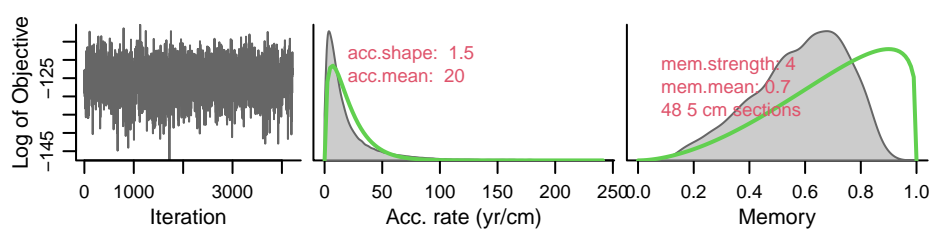


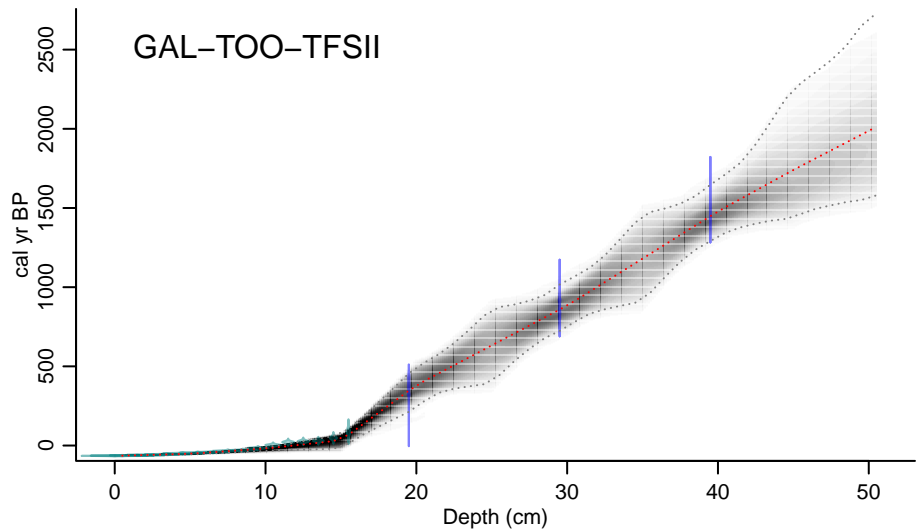
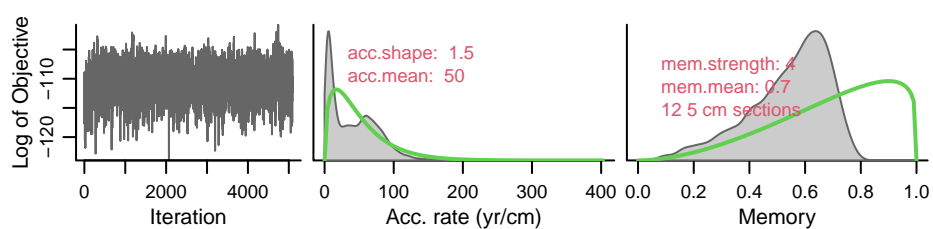


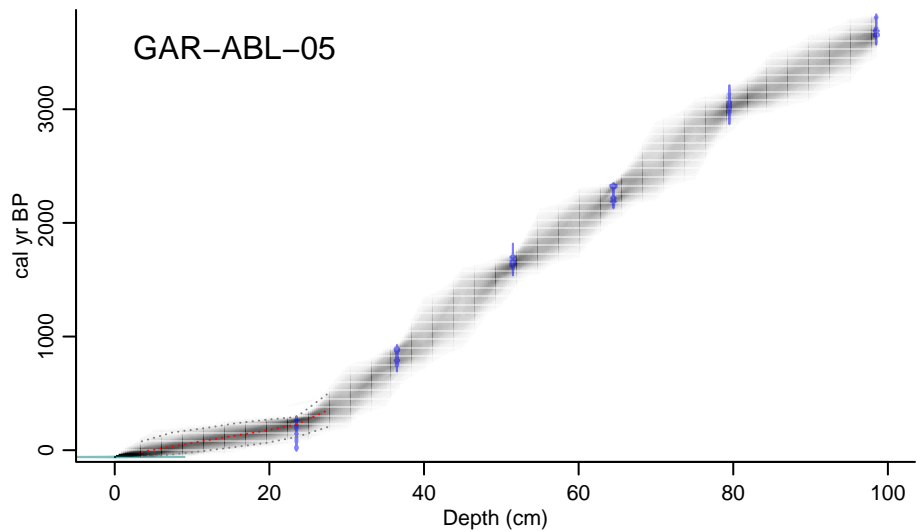
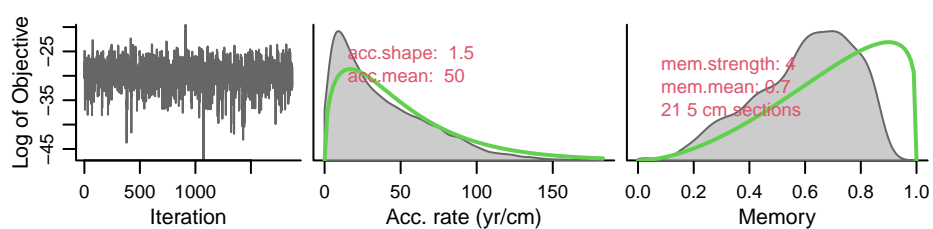
DKL-CHO-J16

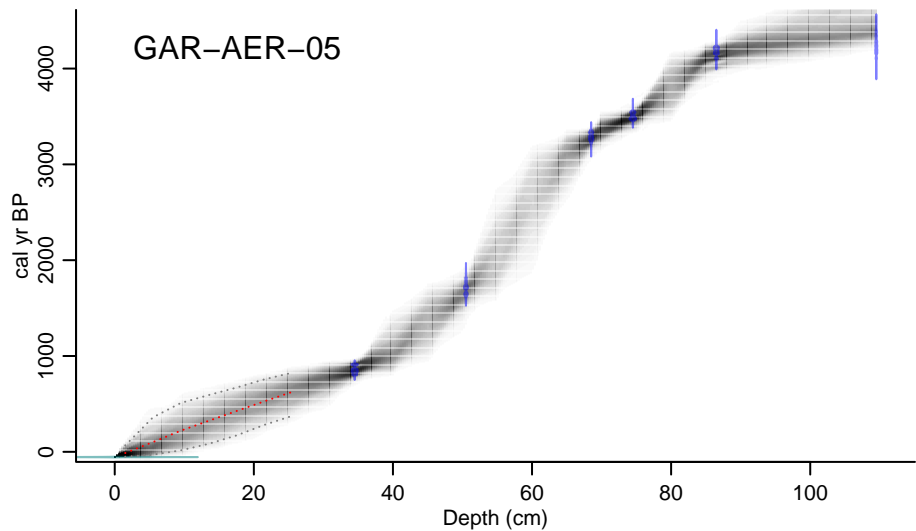
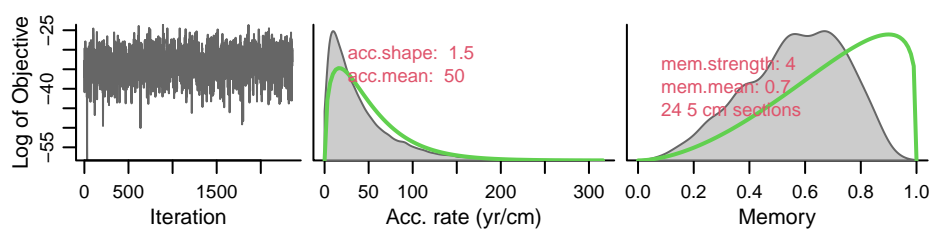


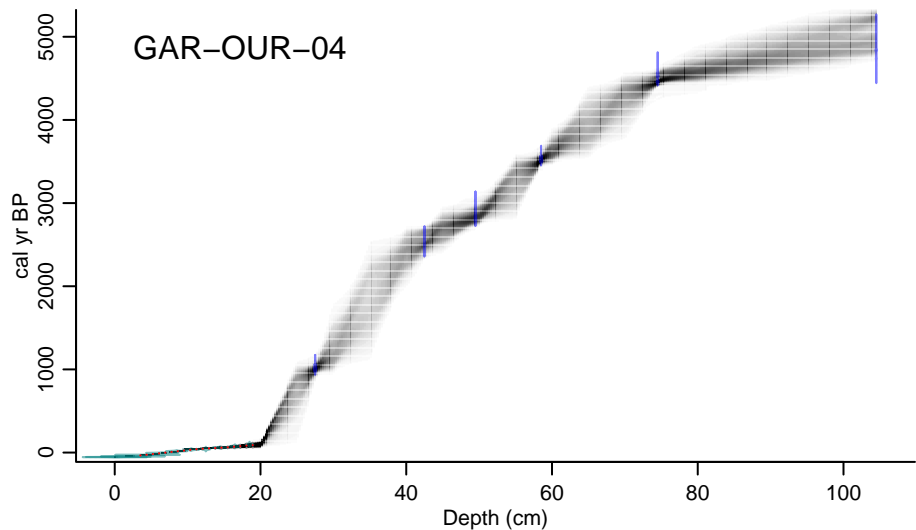
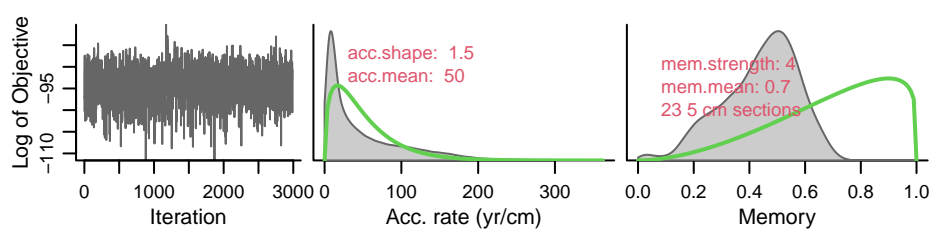


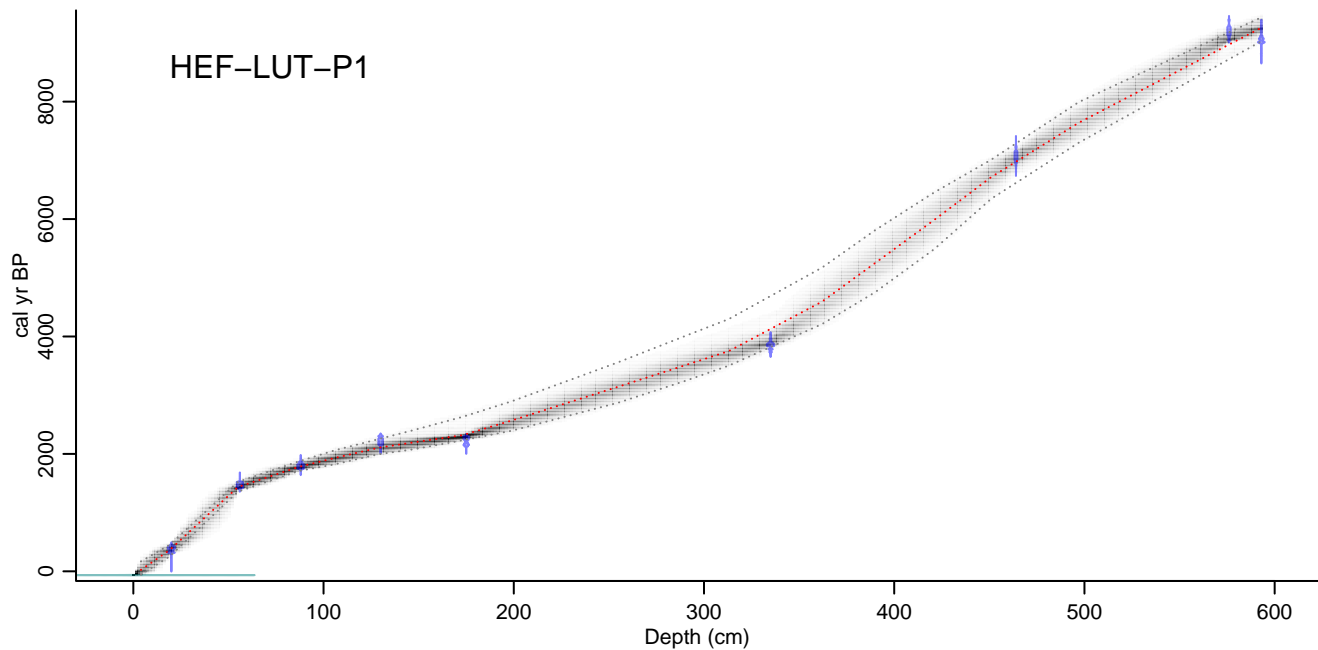
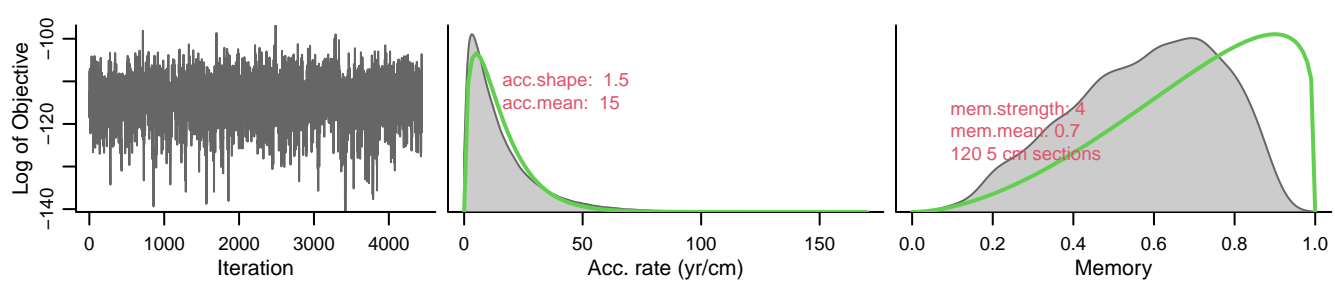


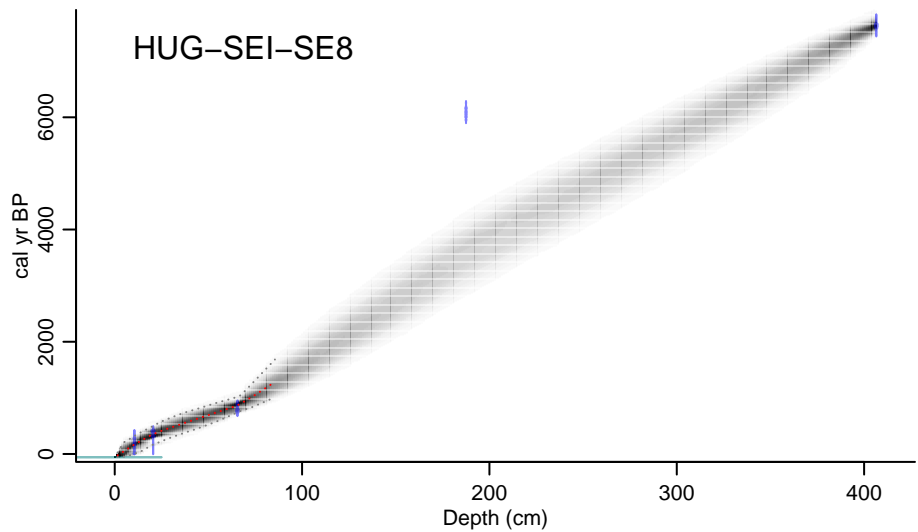
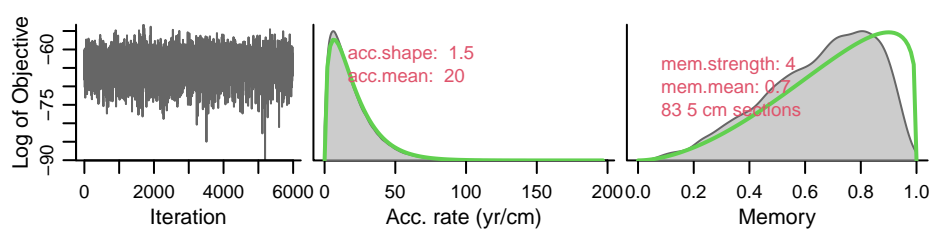


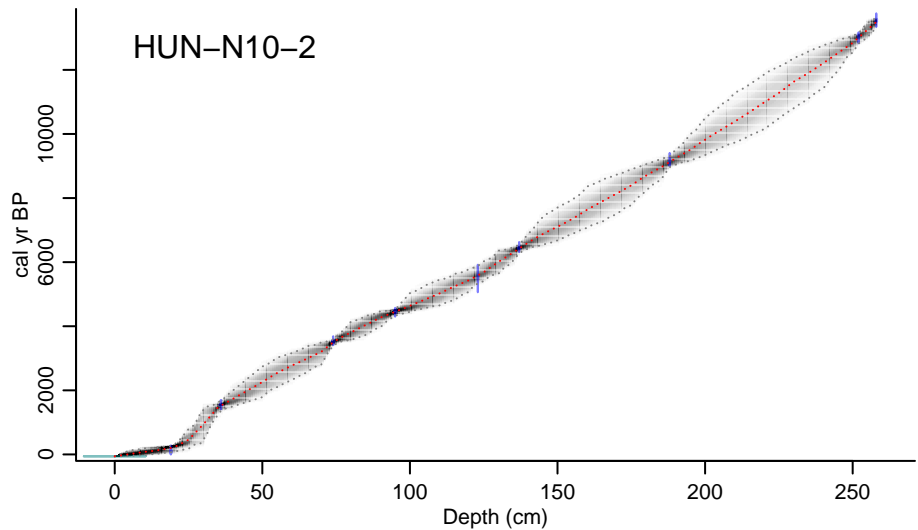
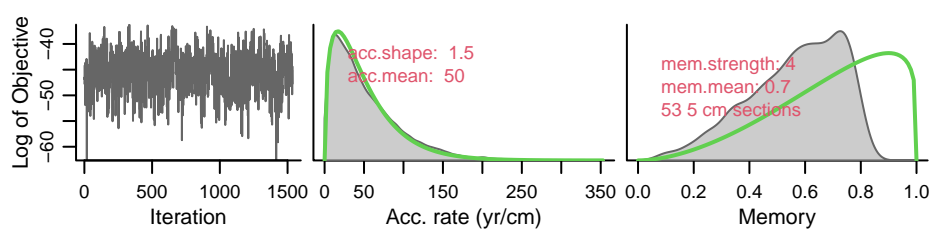




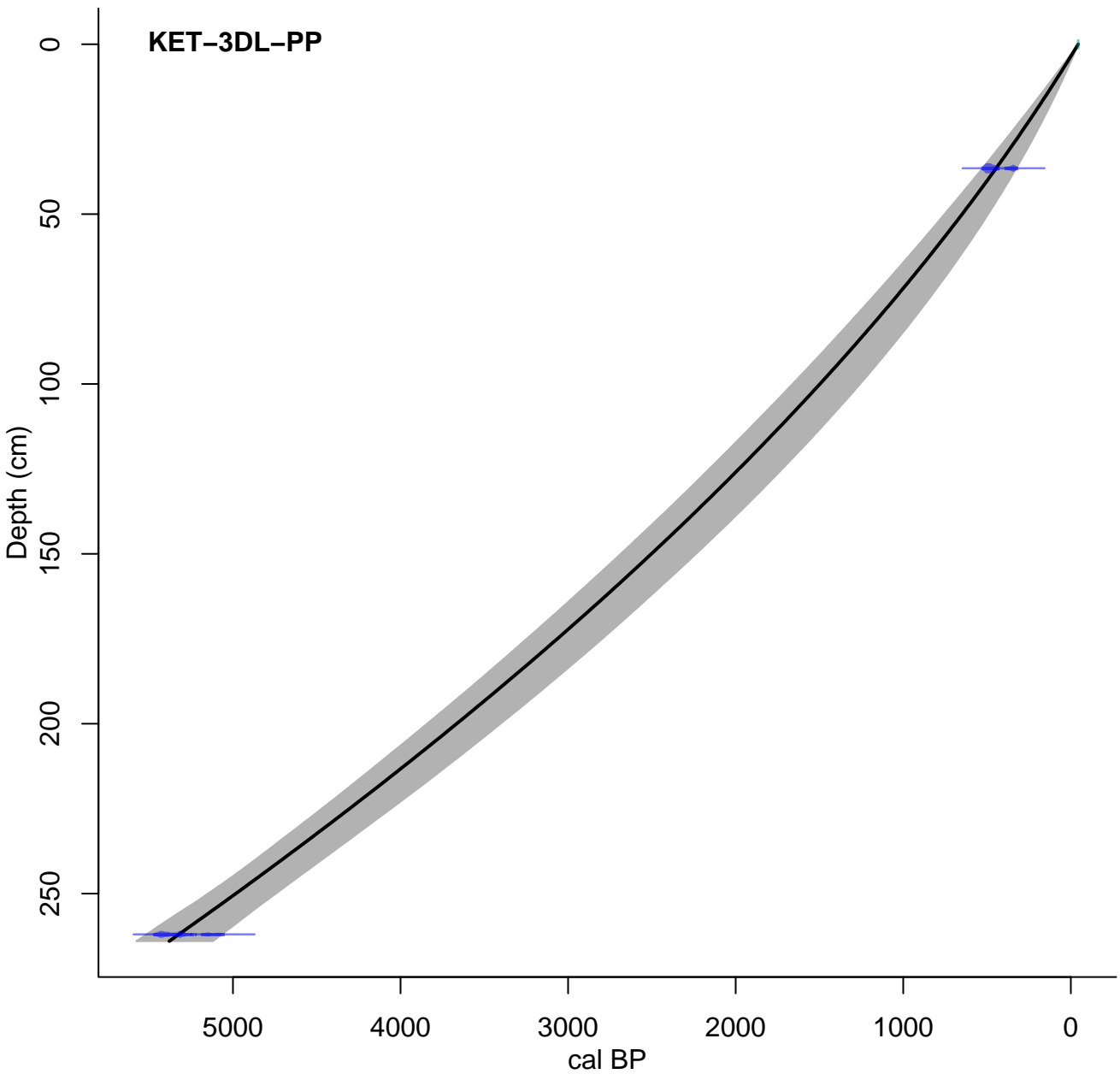


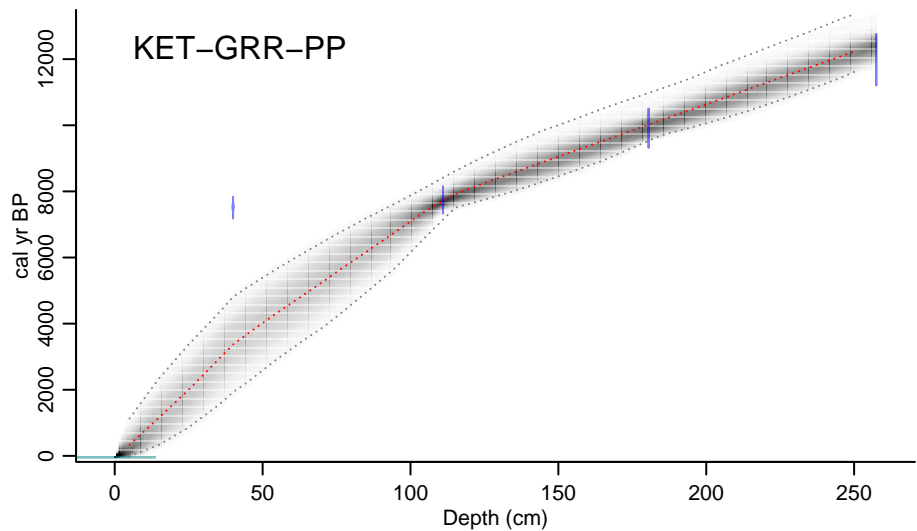
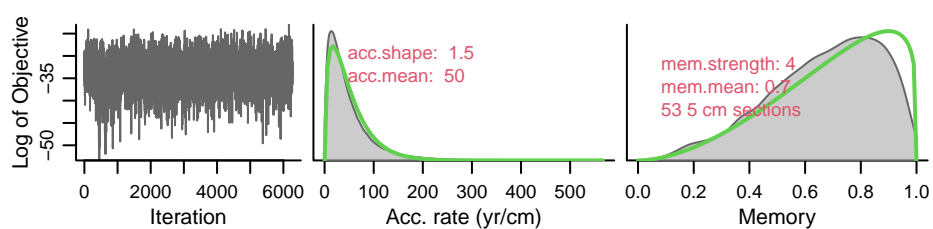


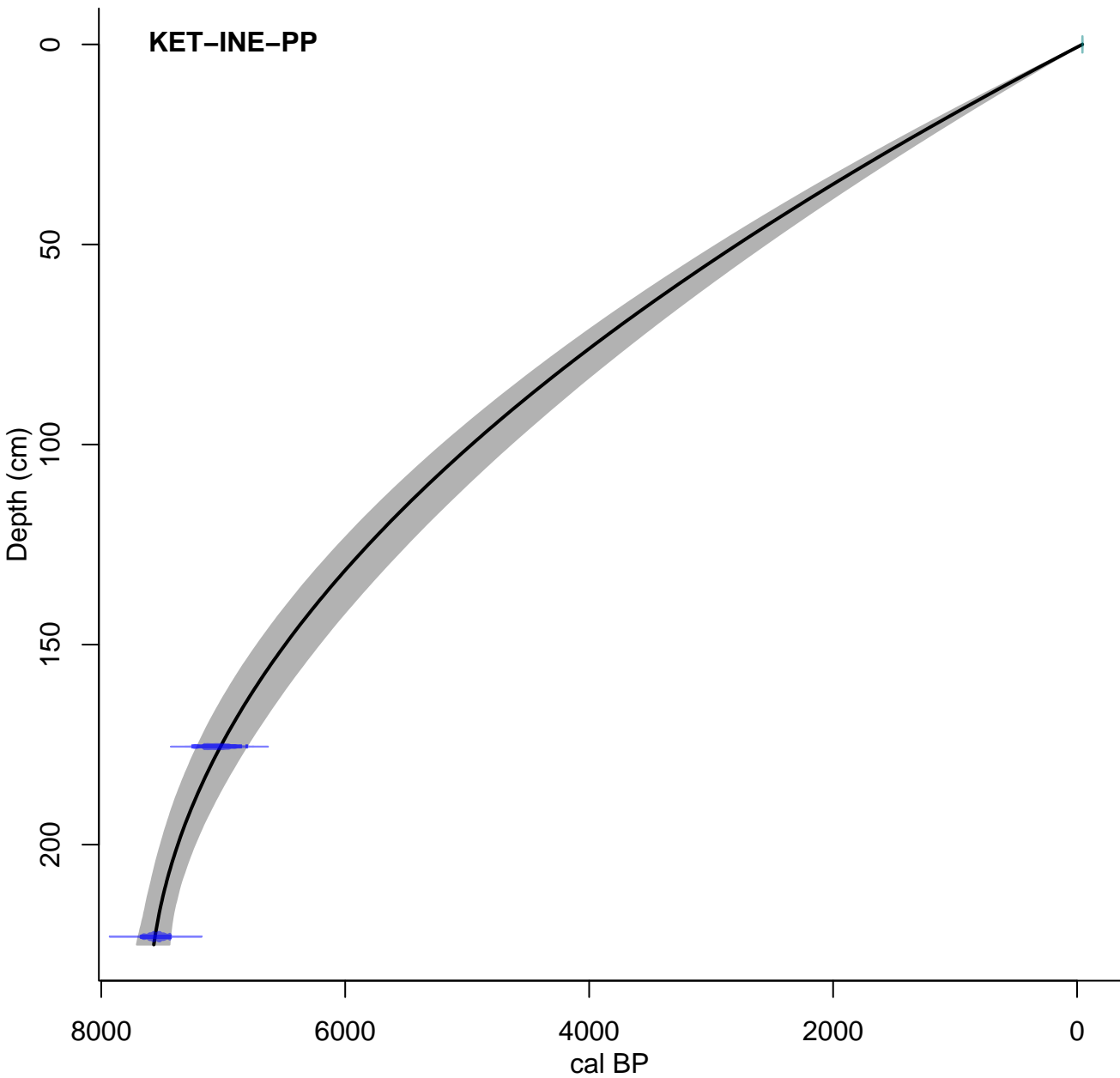


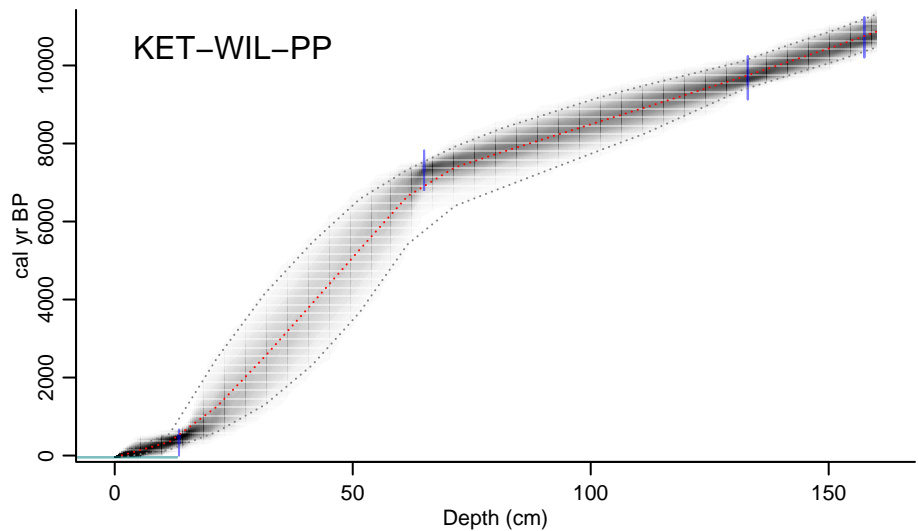
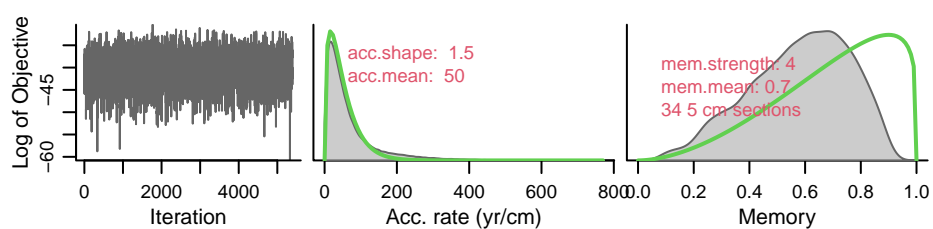


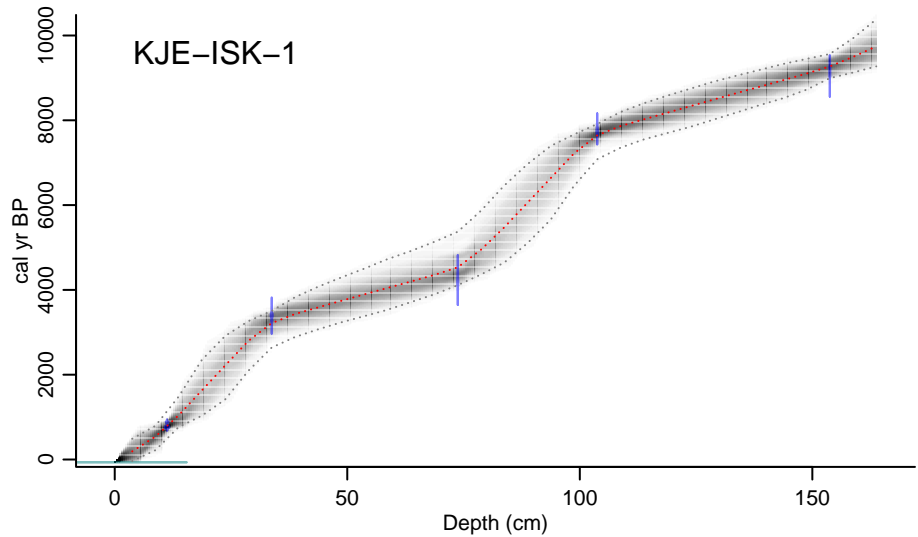
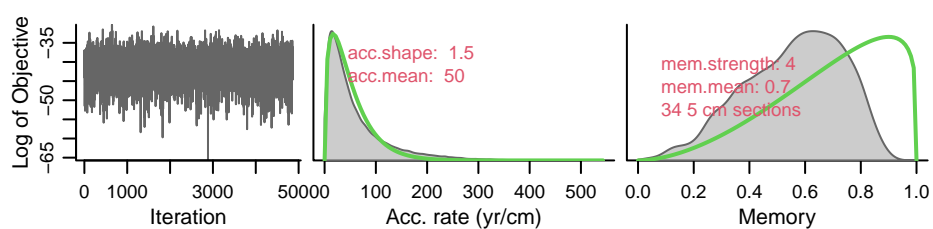
KET-3DL-PP

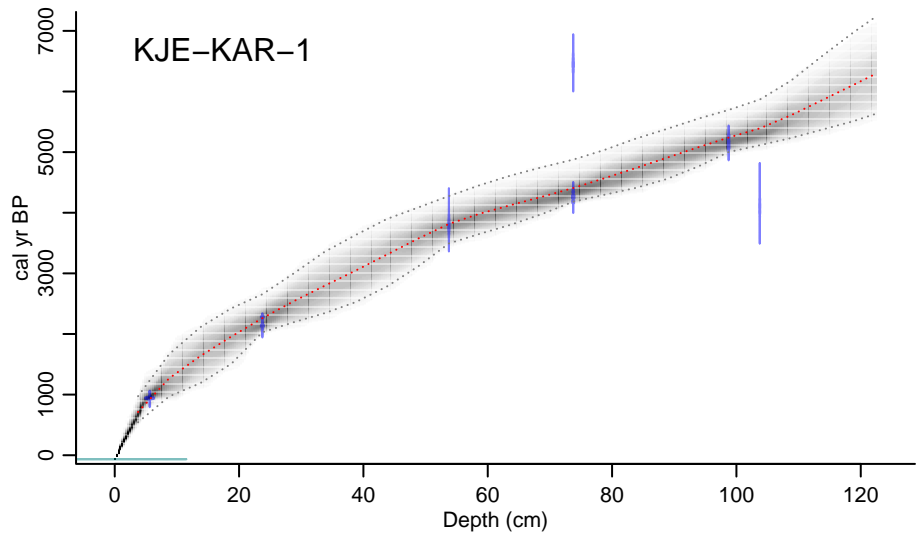
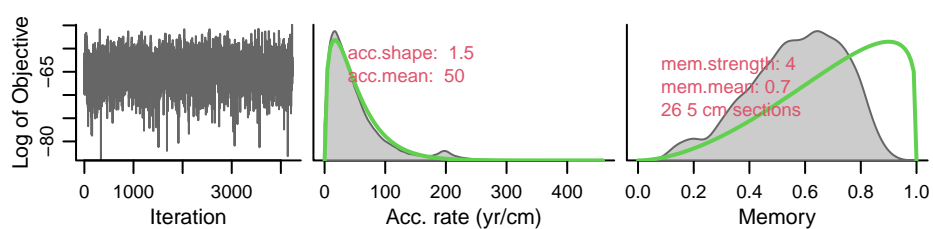


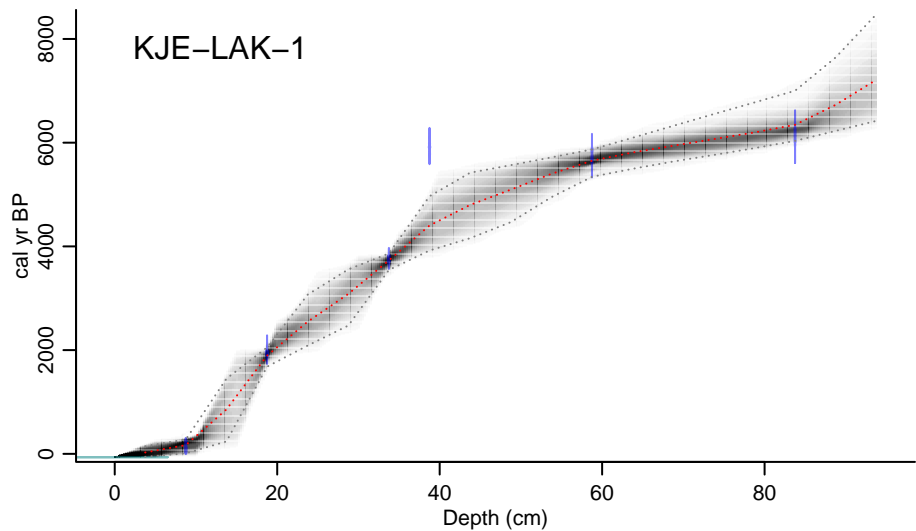
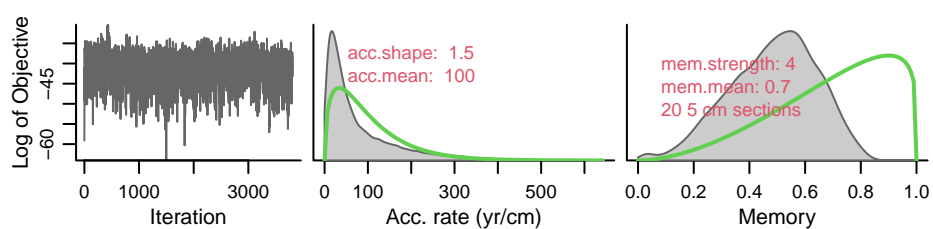


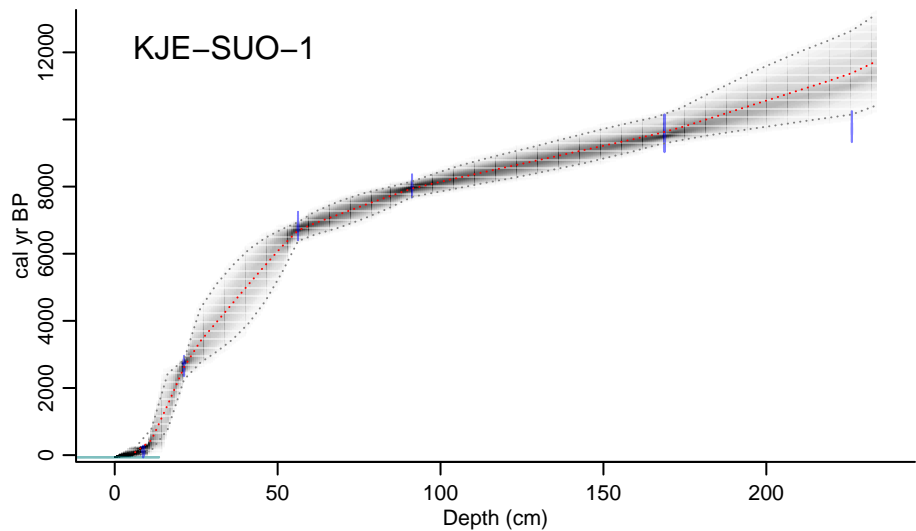
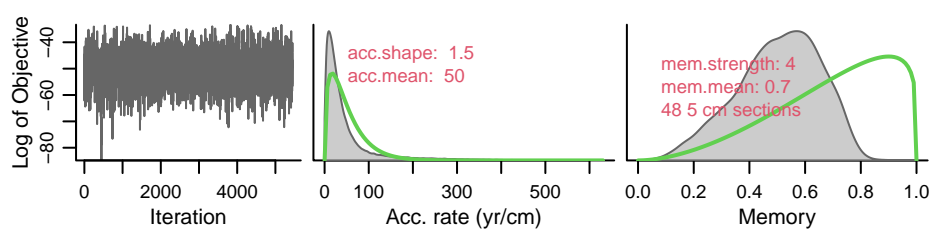


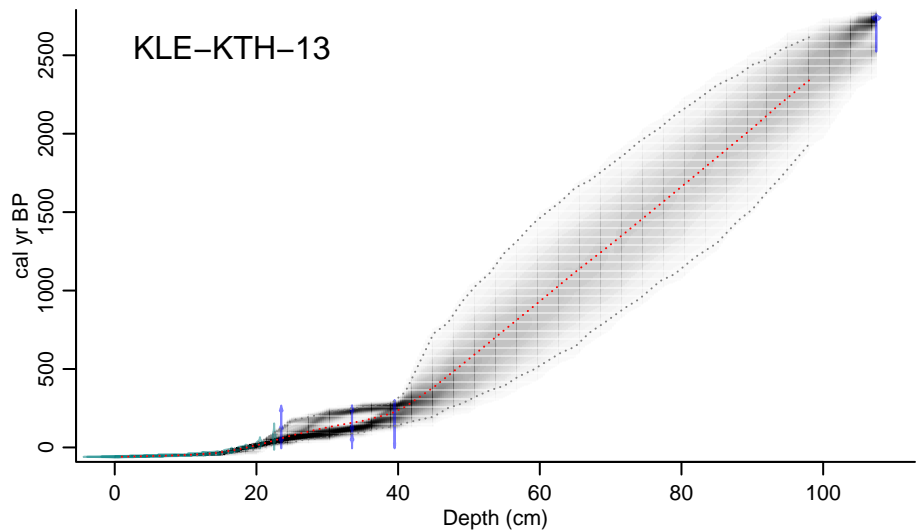
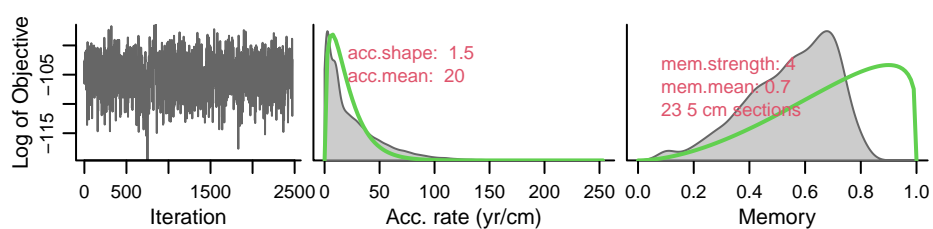


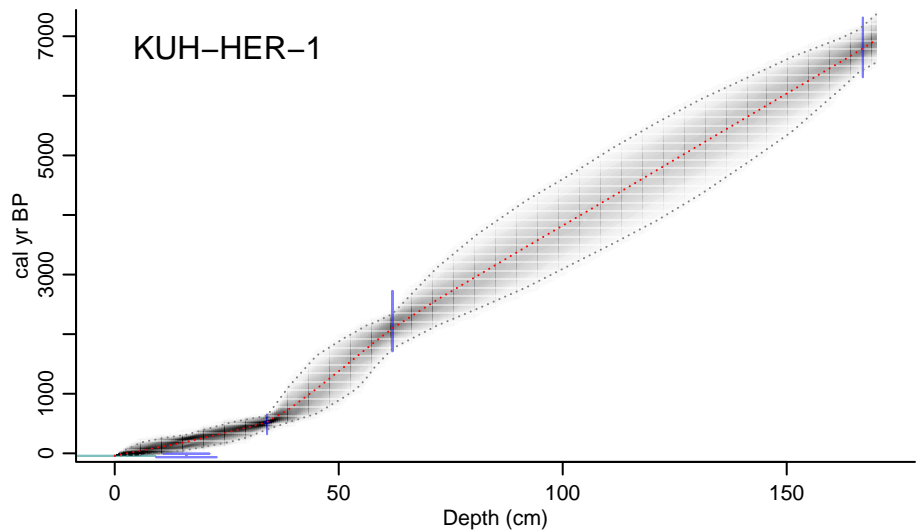
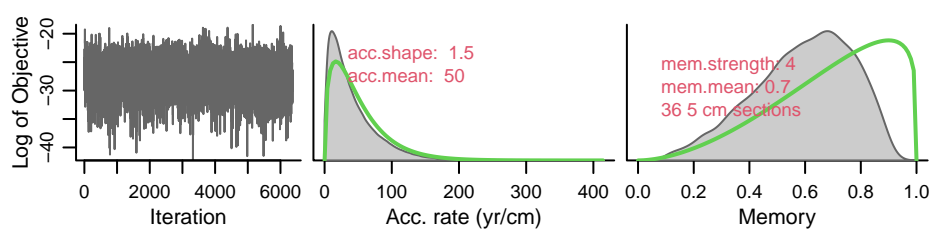


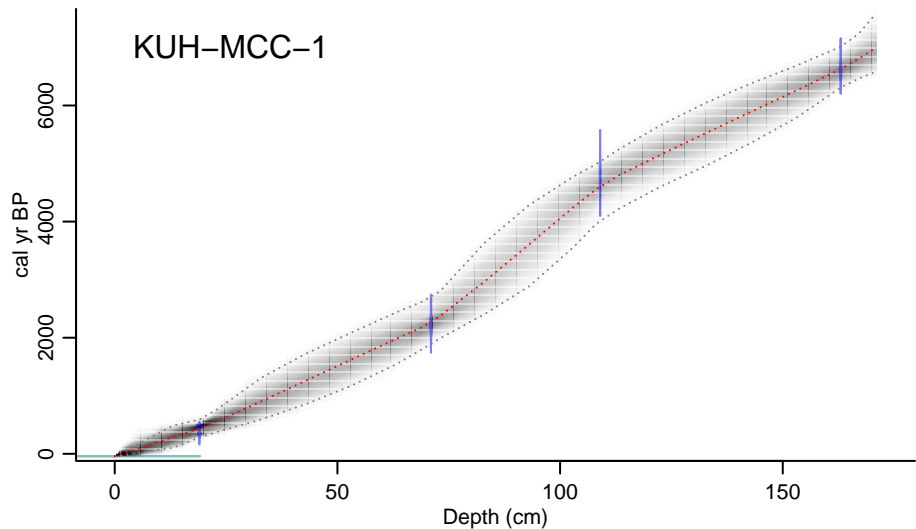
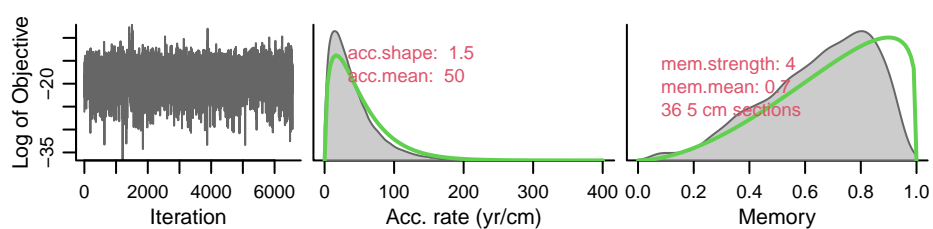


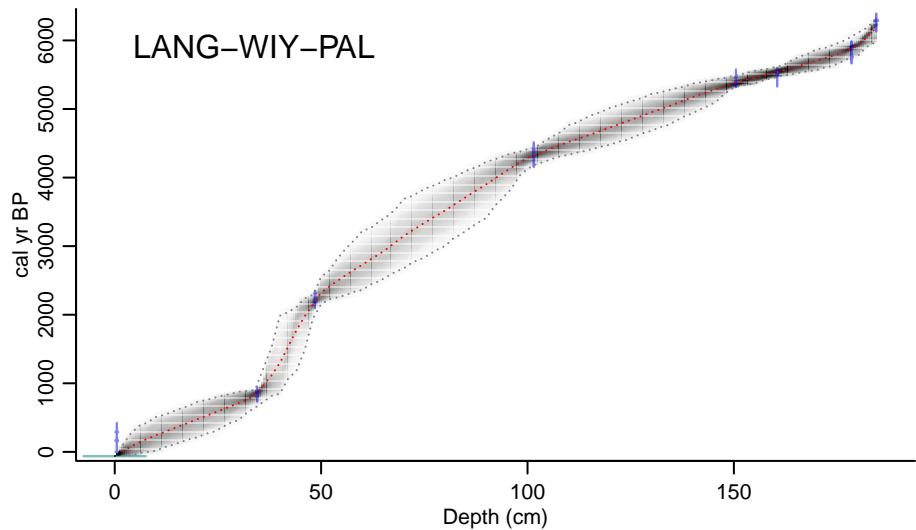
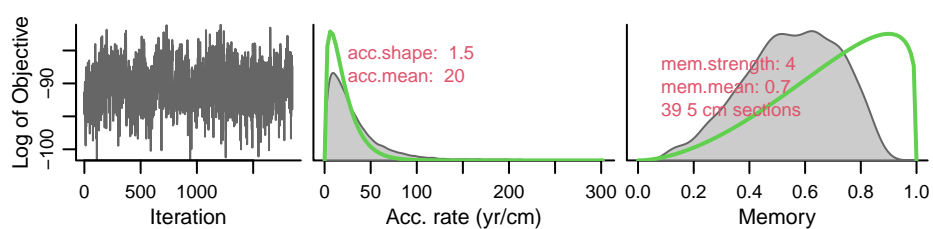




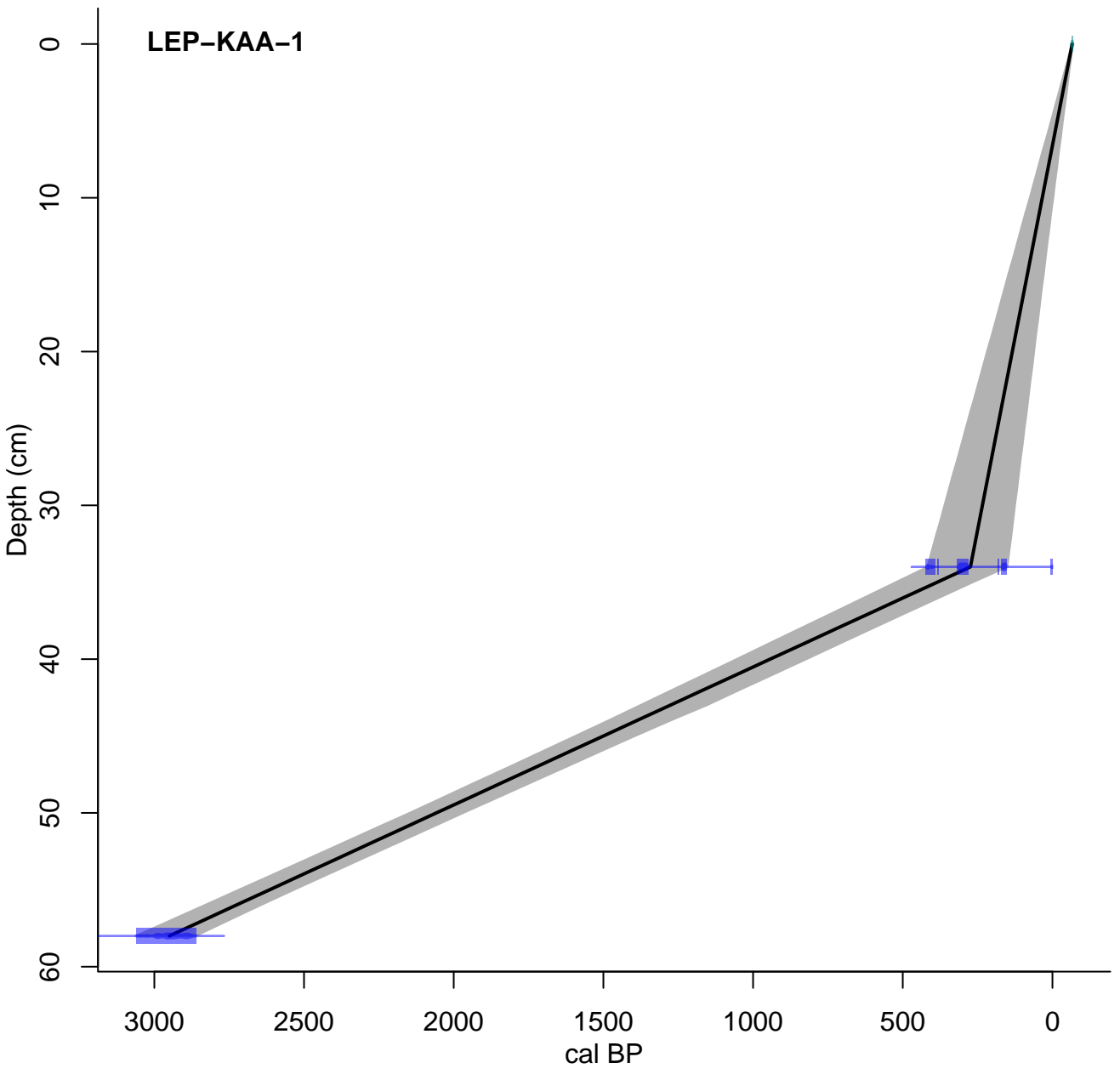




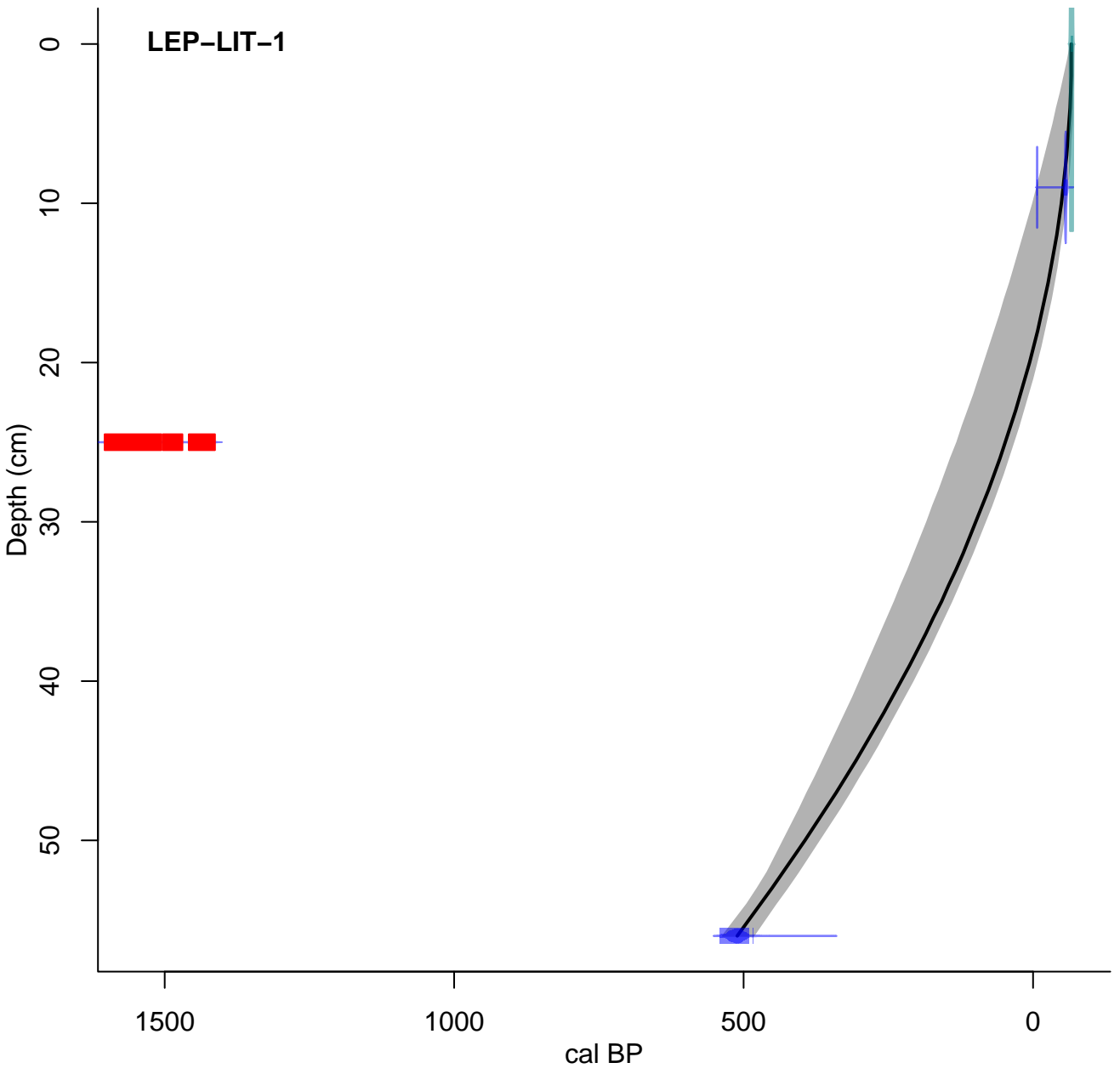


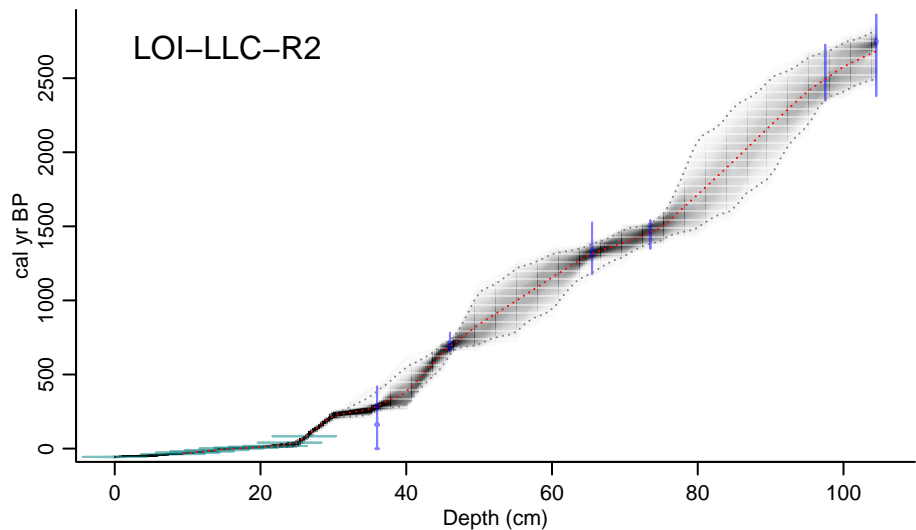
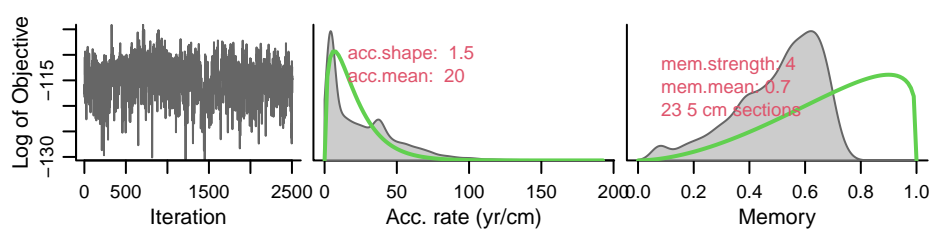


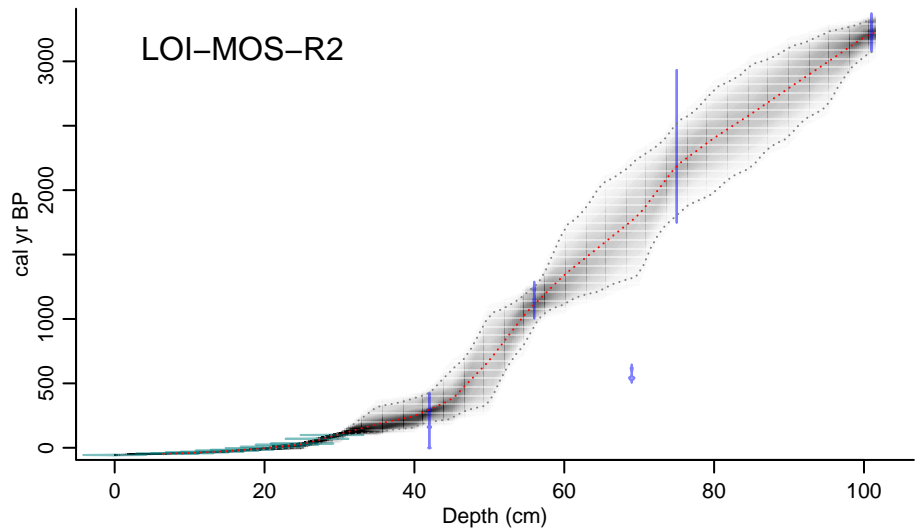
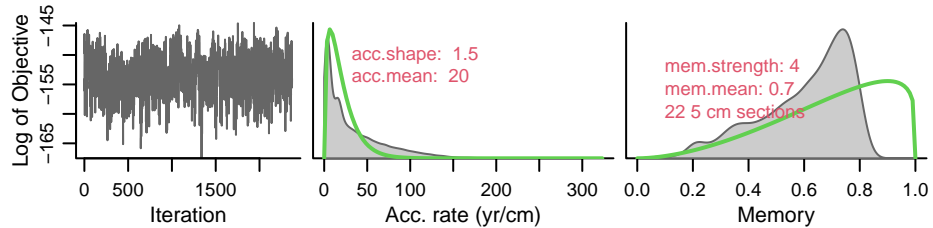
LEP-KAA-1

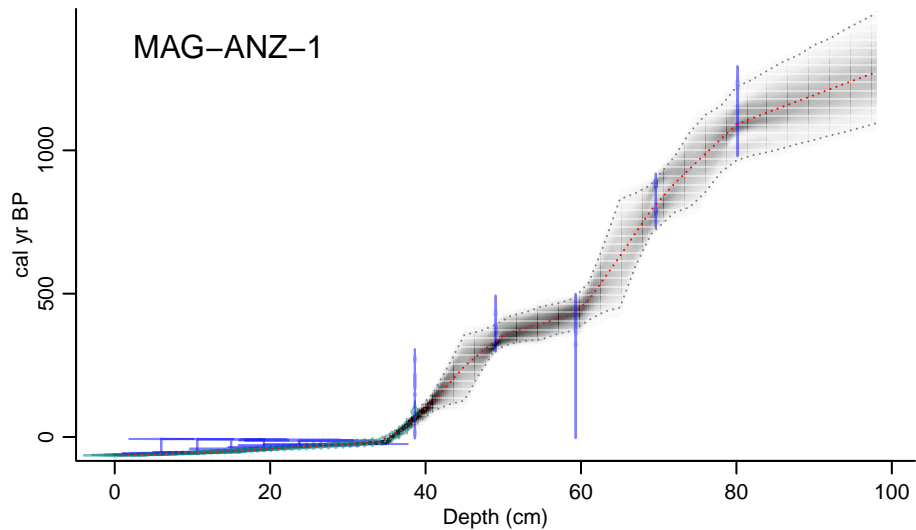
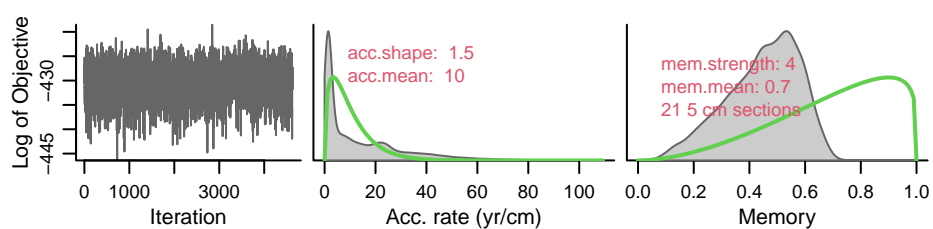


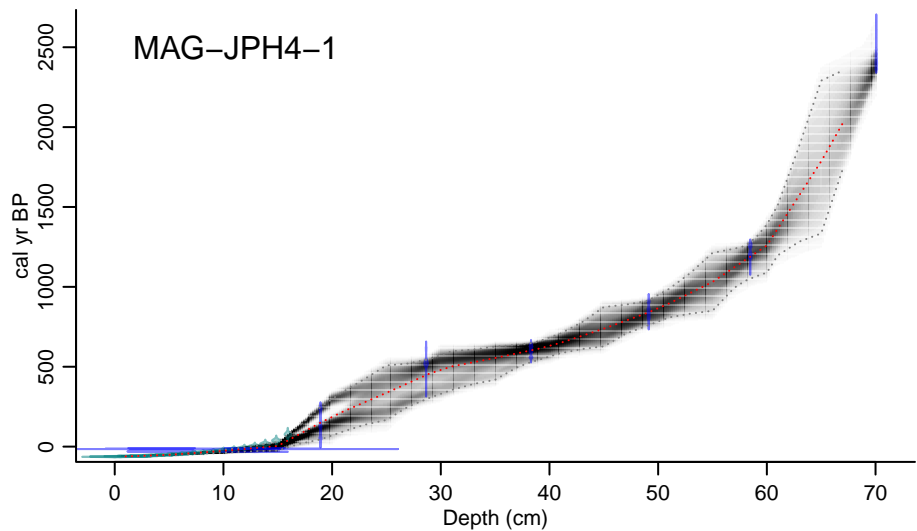
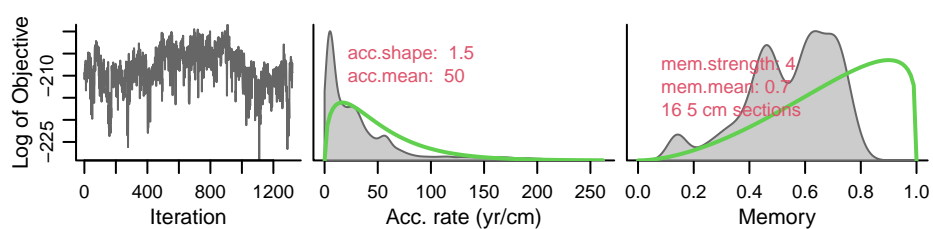
LEP-LIT-1

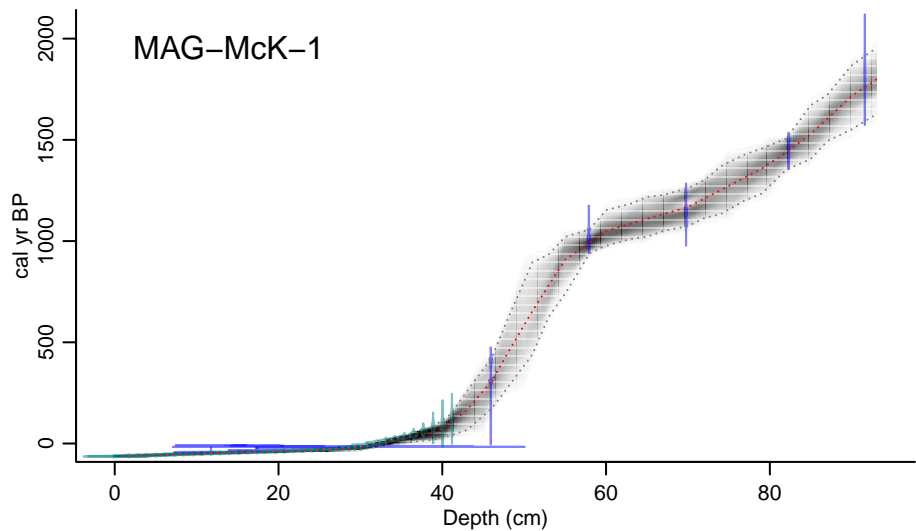
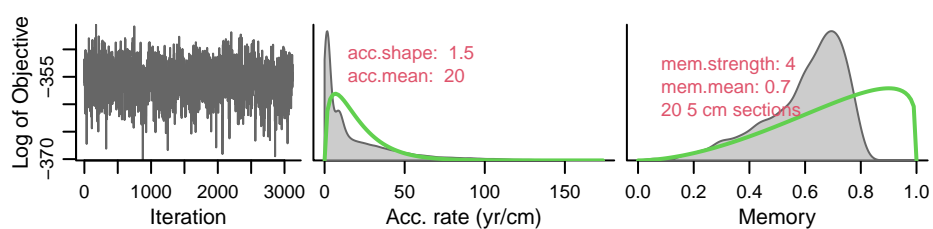


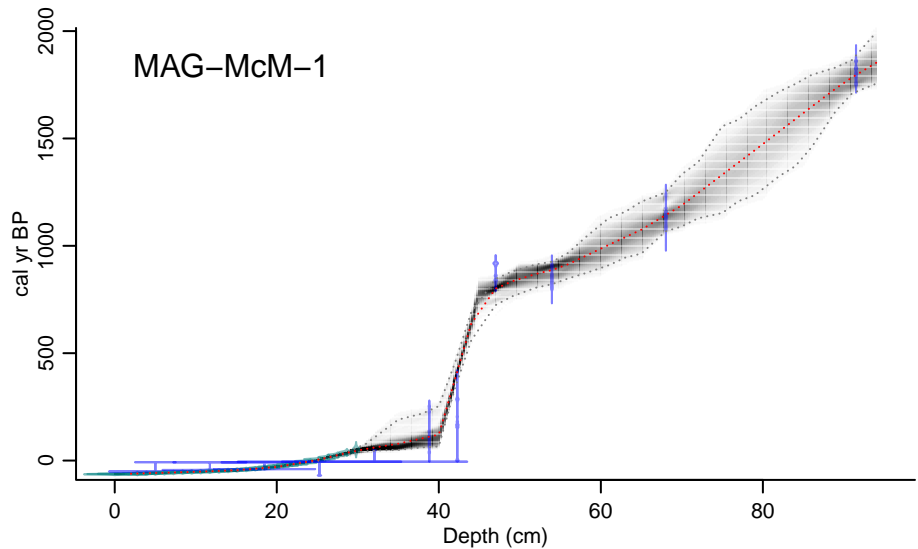
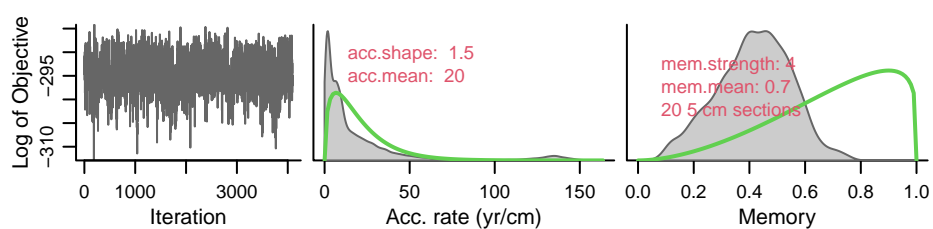


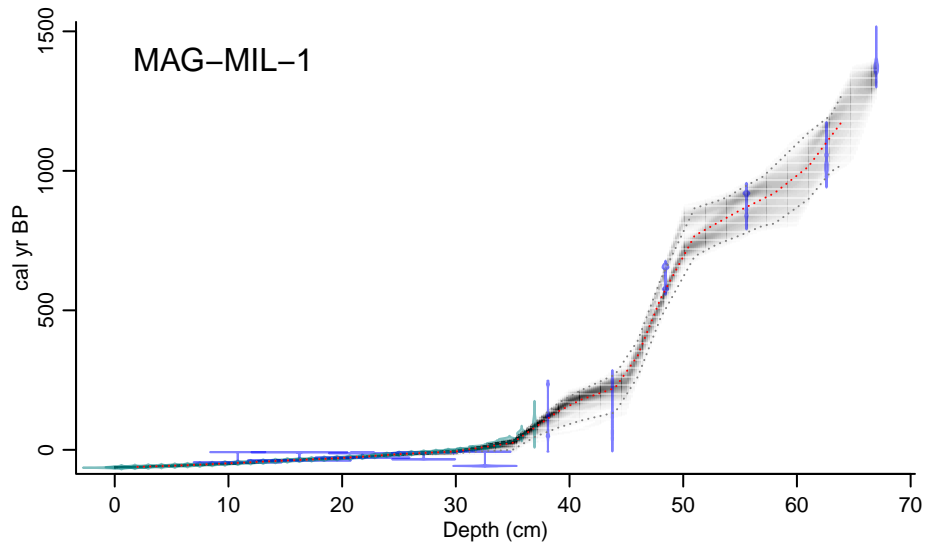
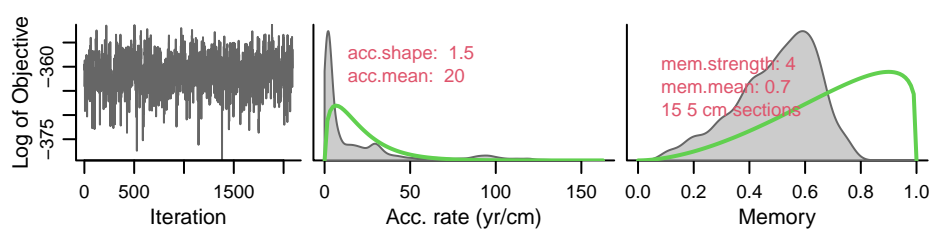


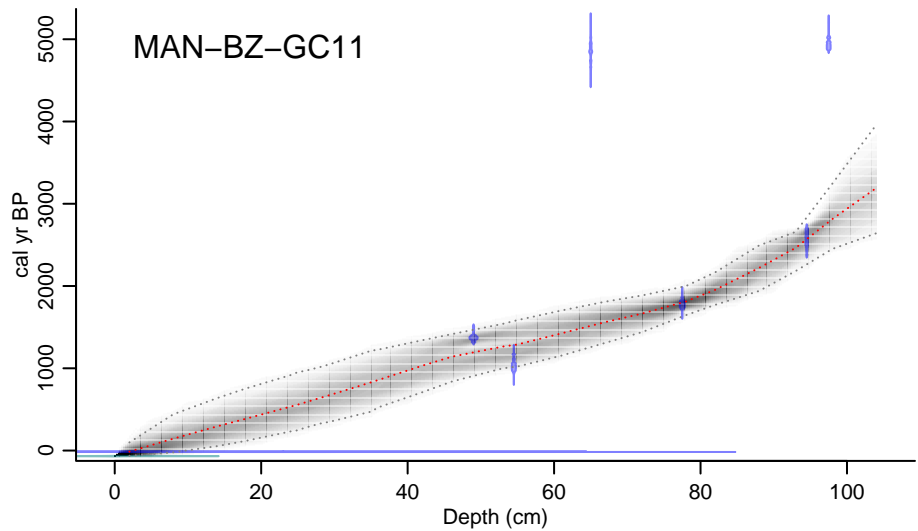
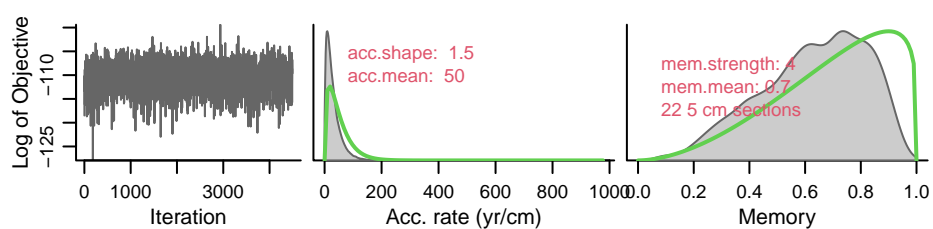




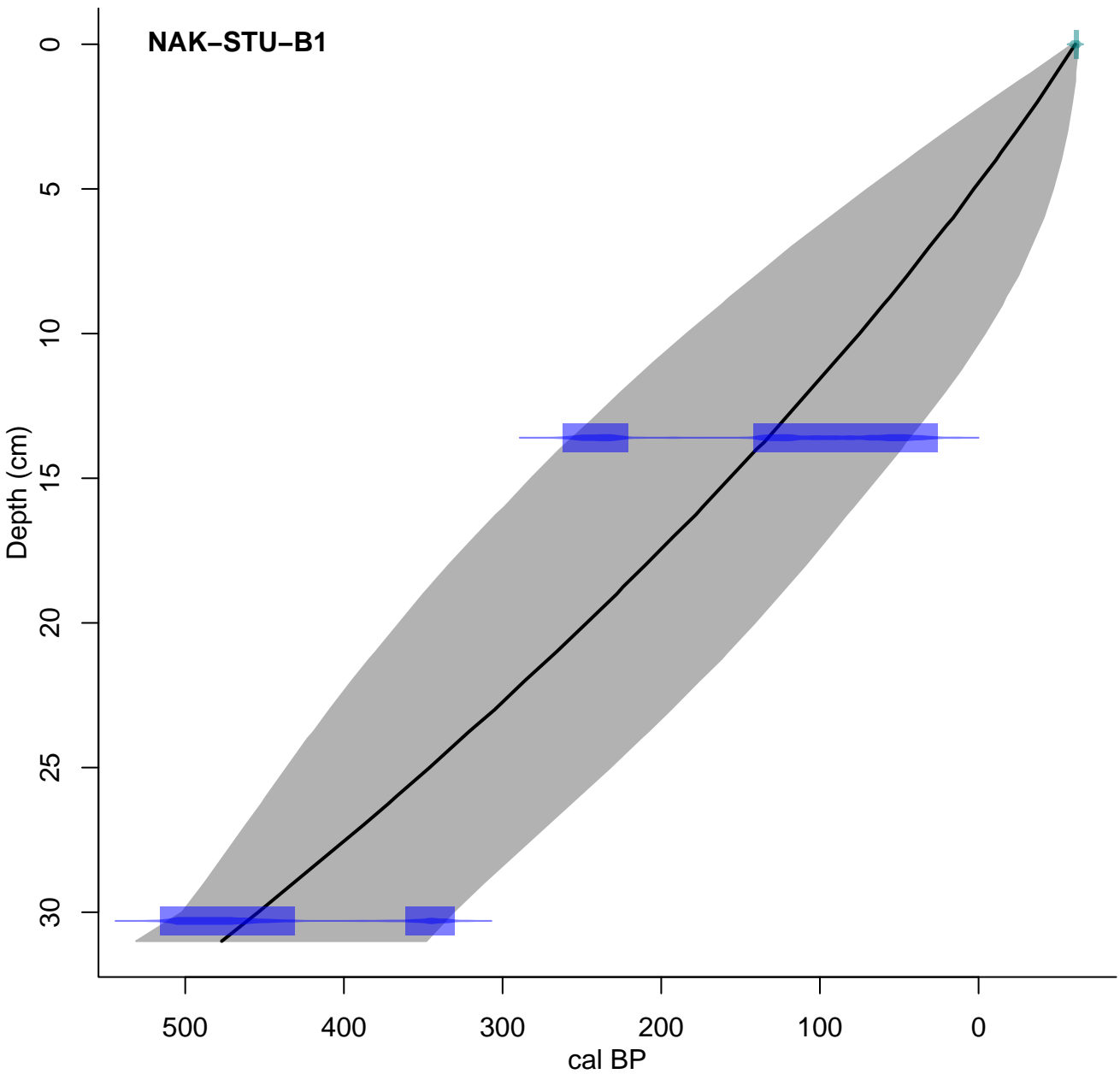


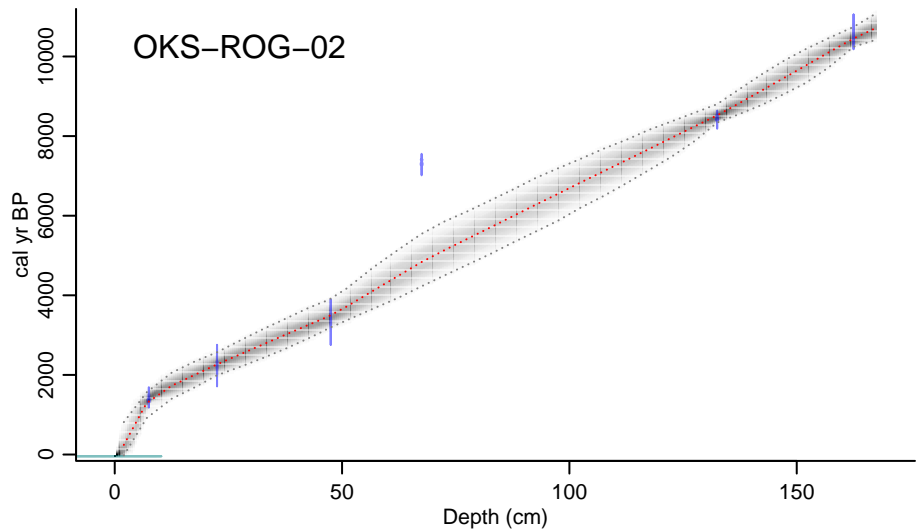
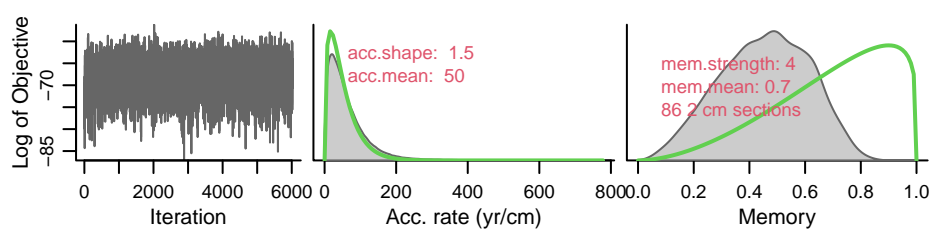


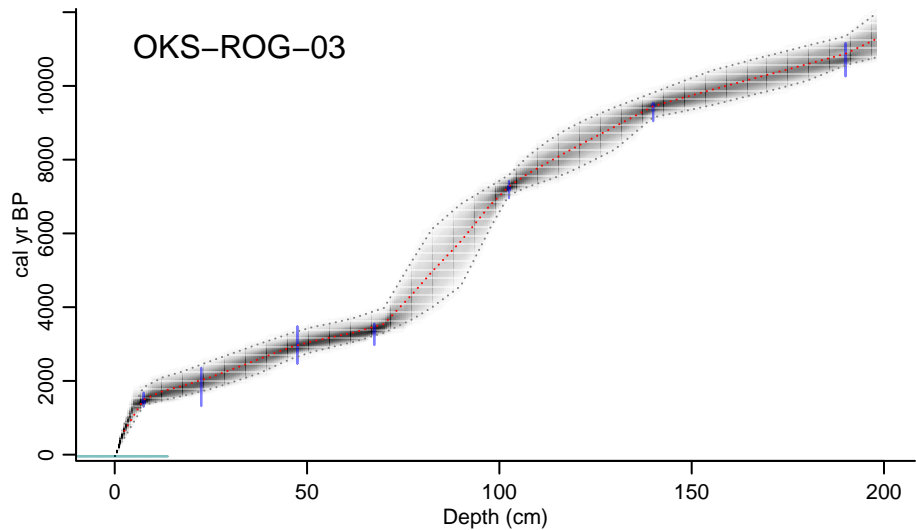
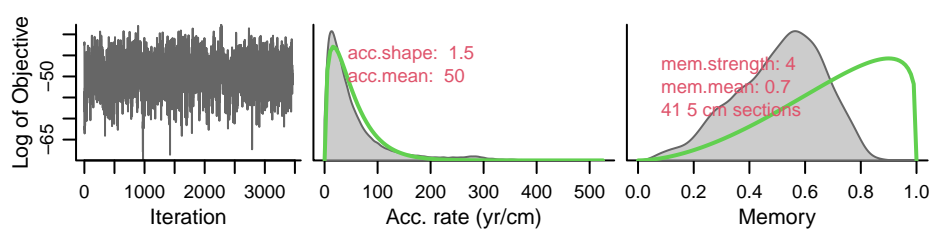


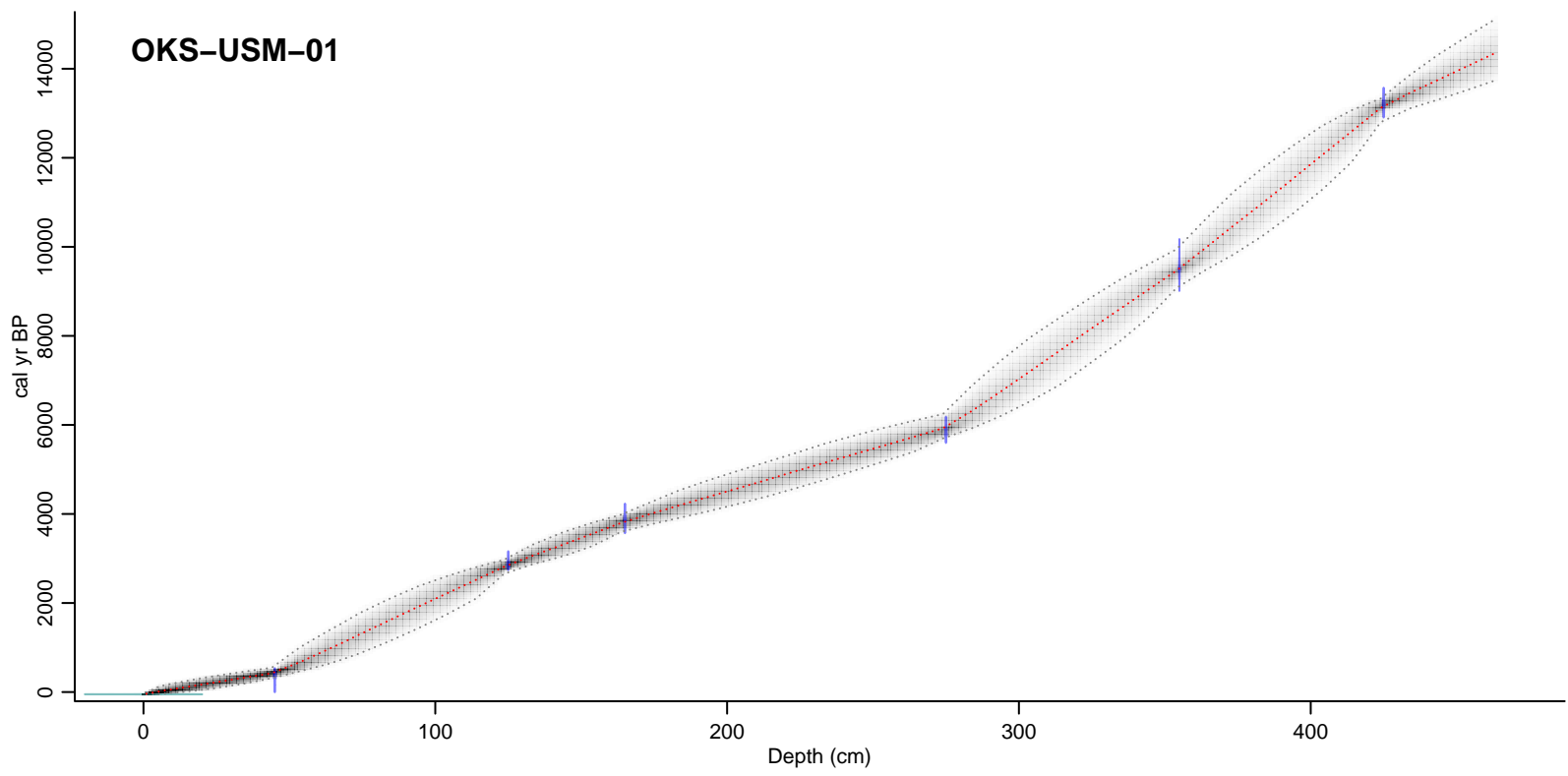
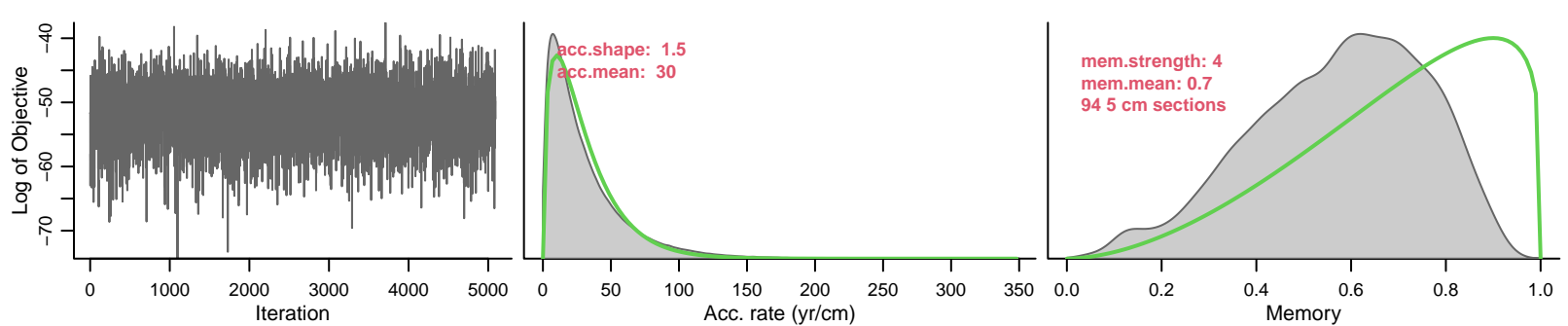


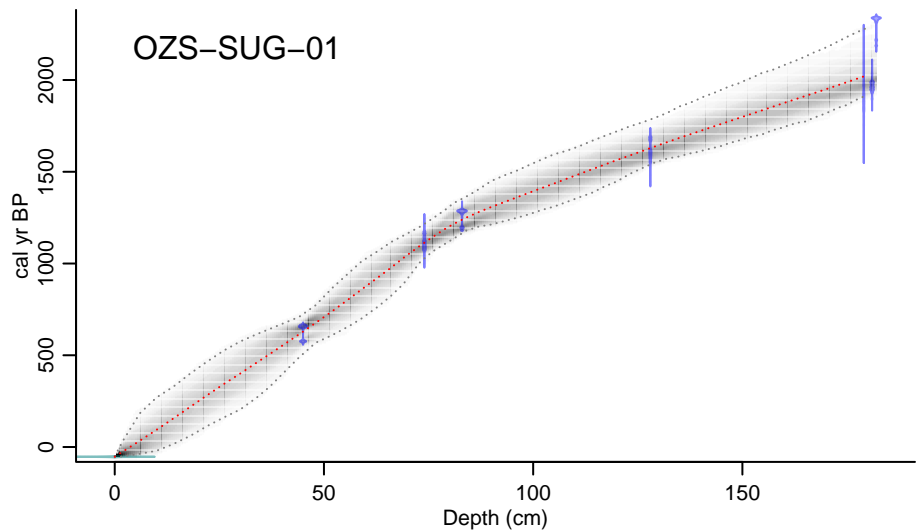
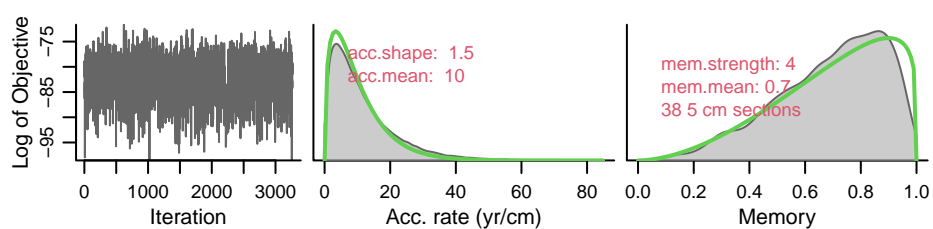
NAK-STU-B1

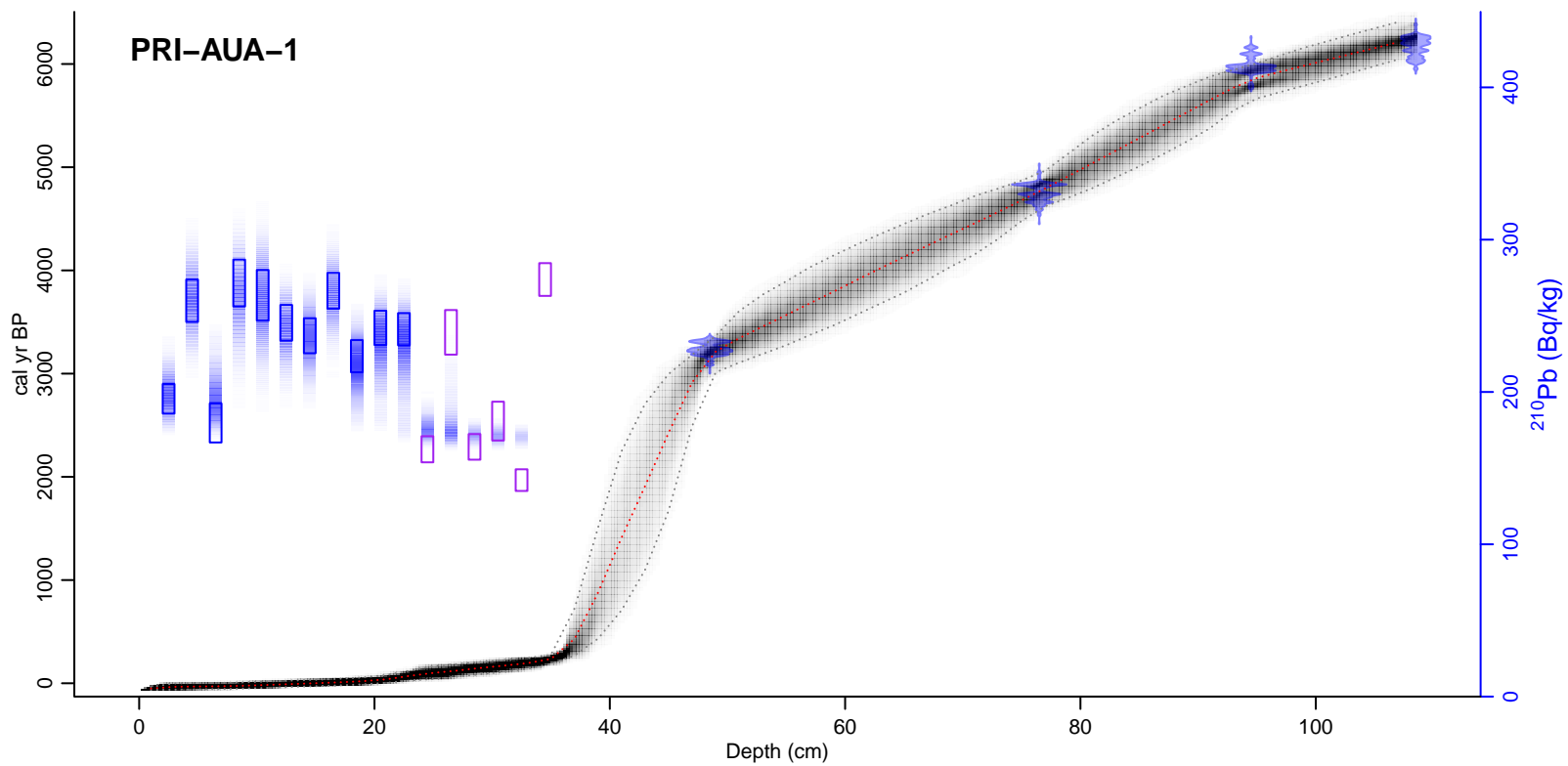
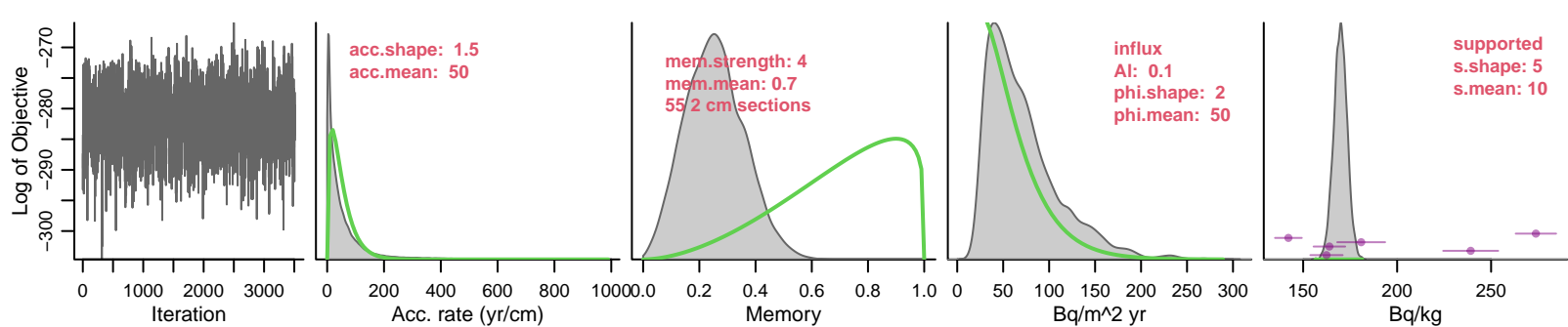


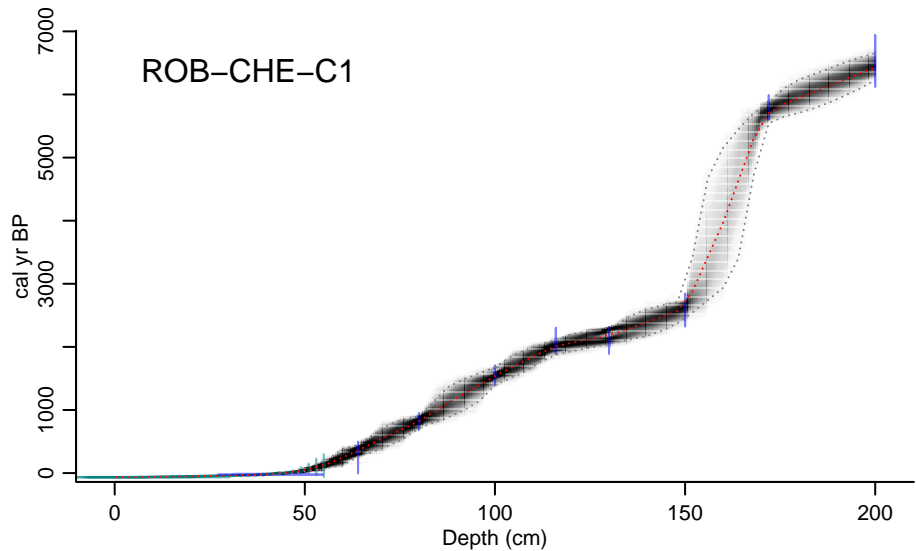
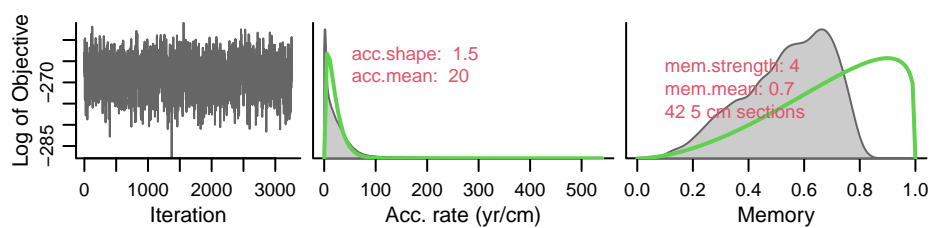


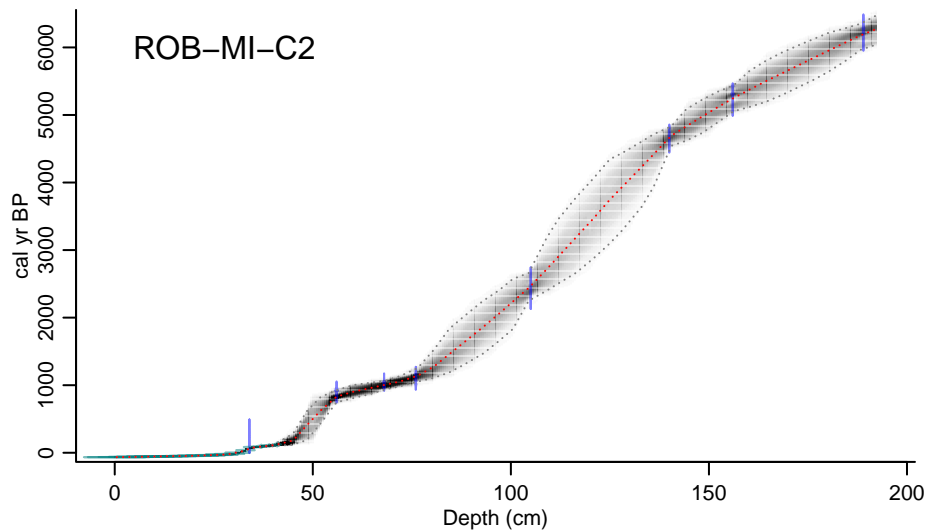
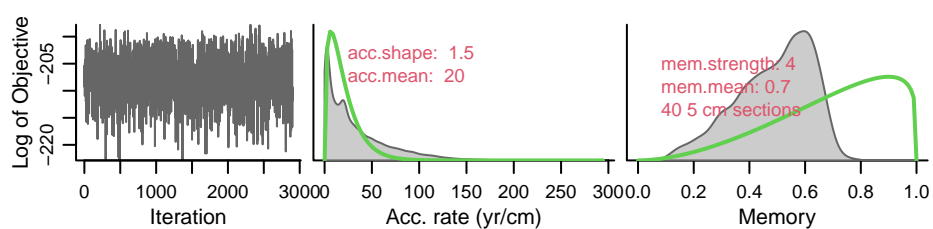


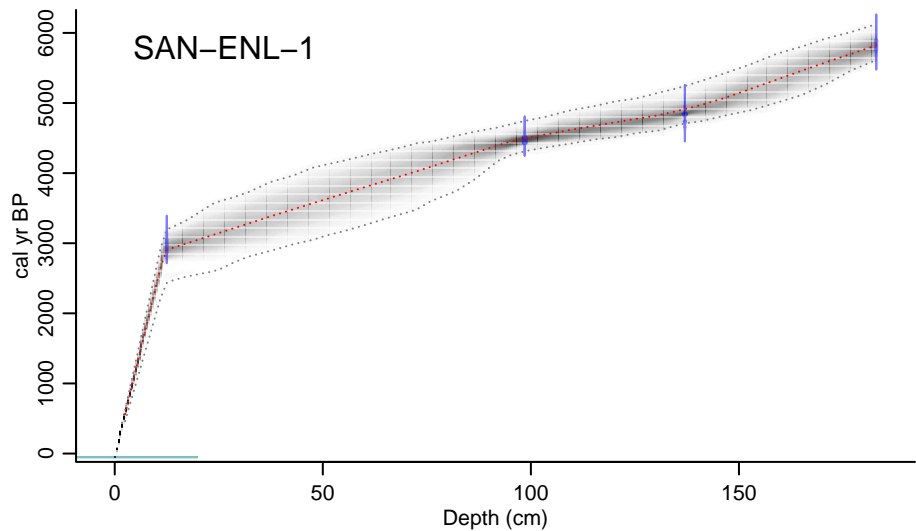
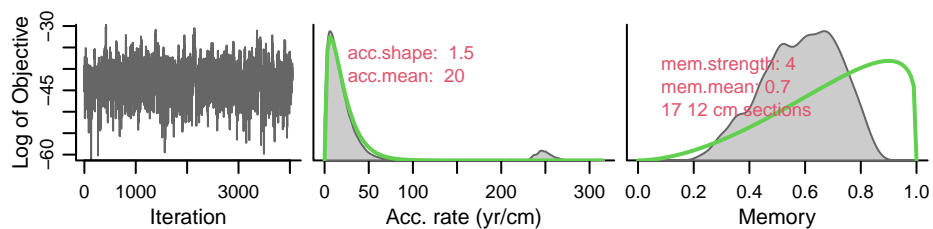


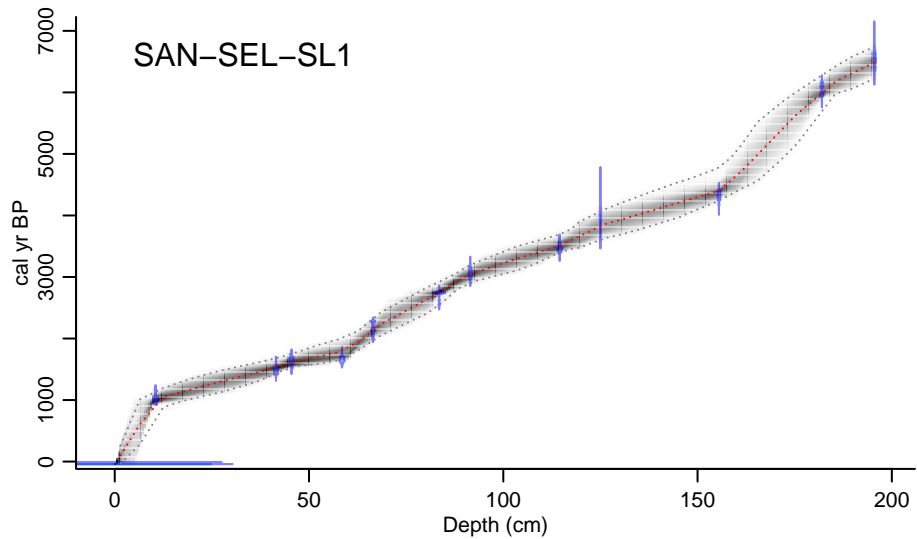
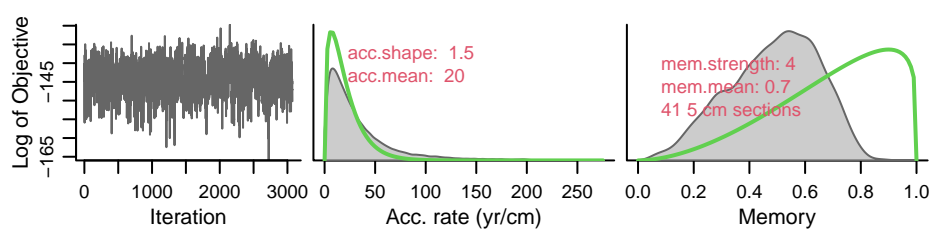


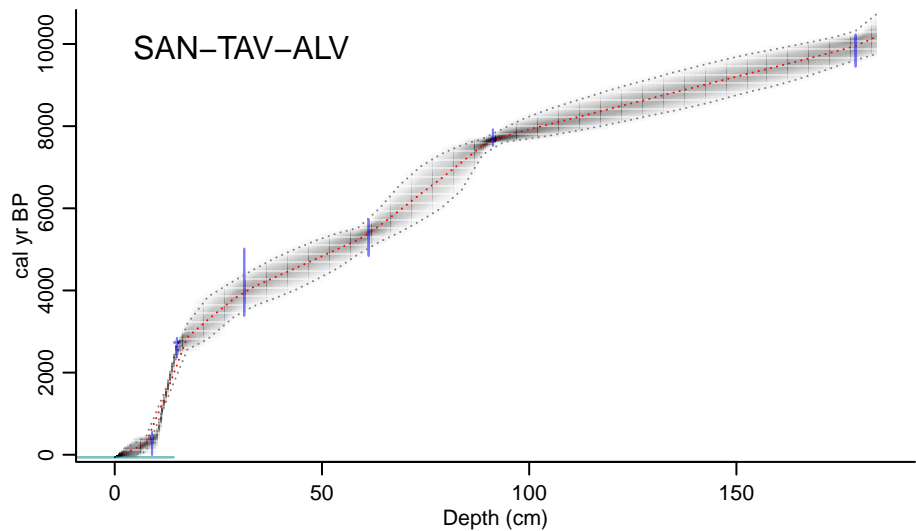
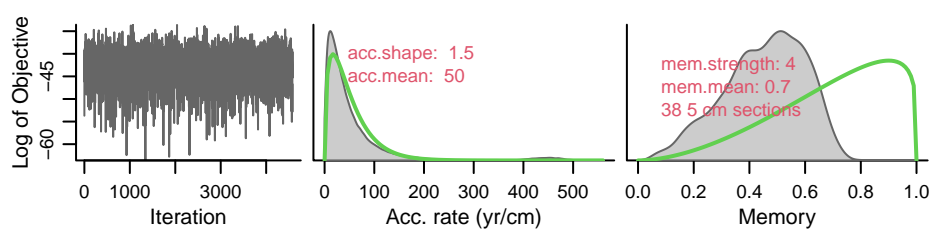


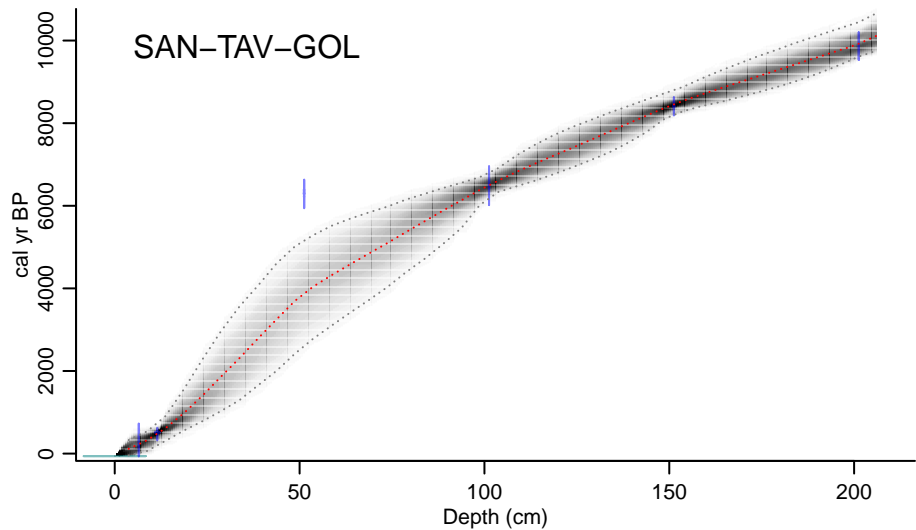
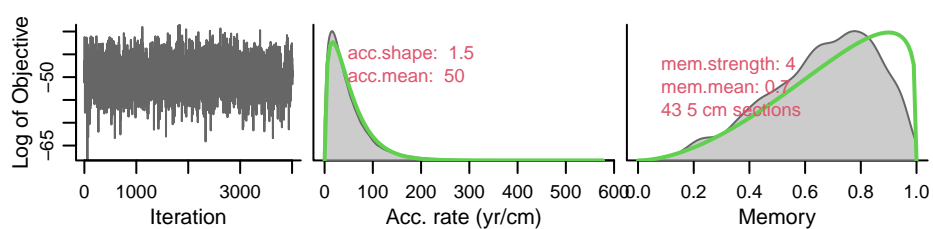


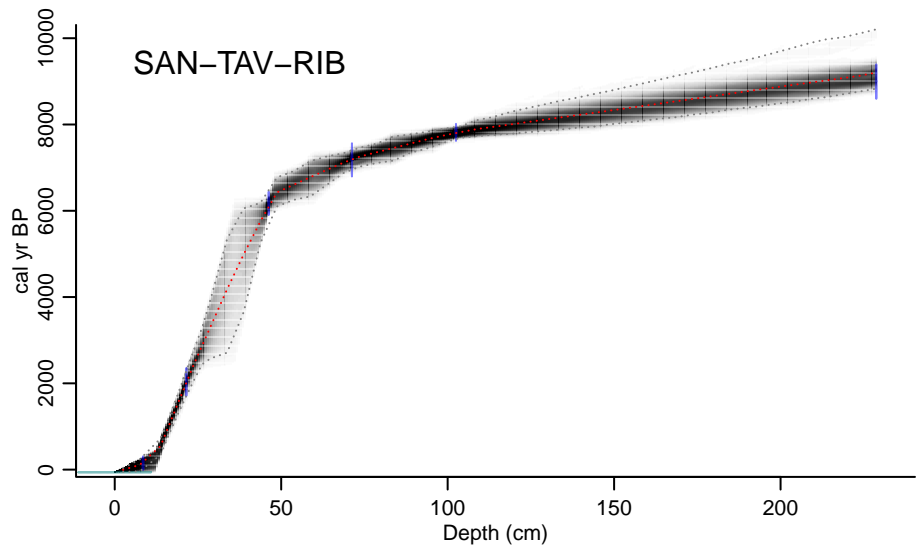
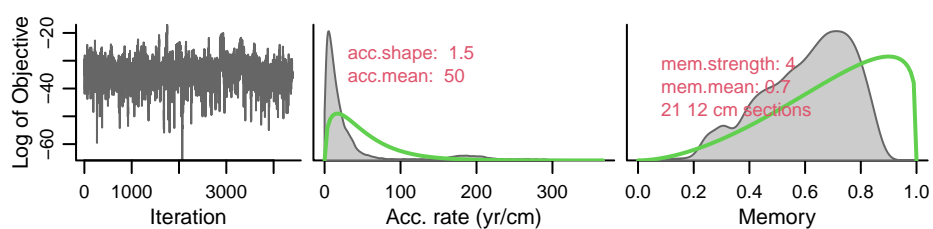


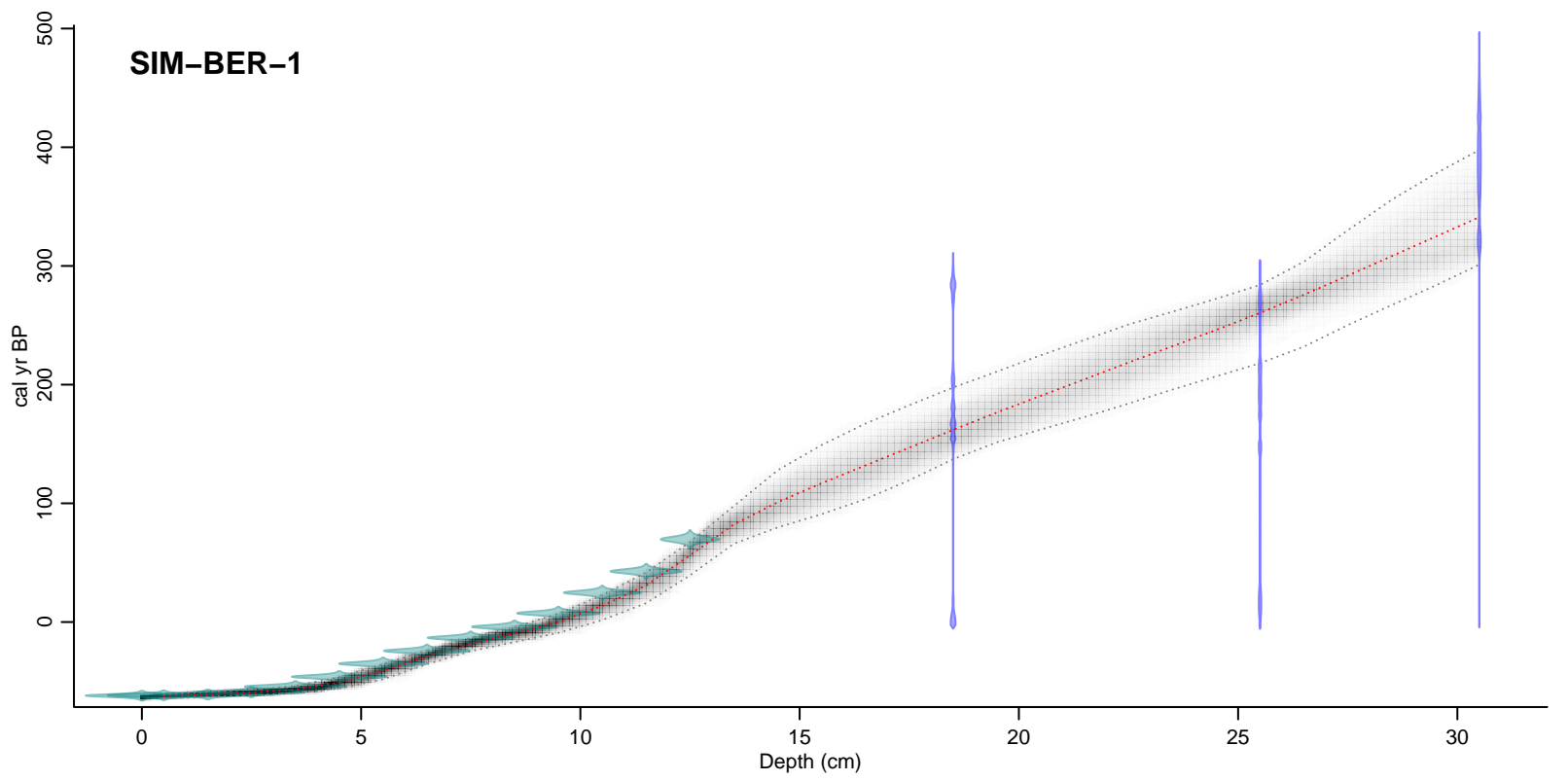
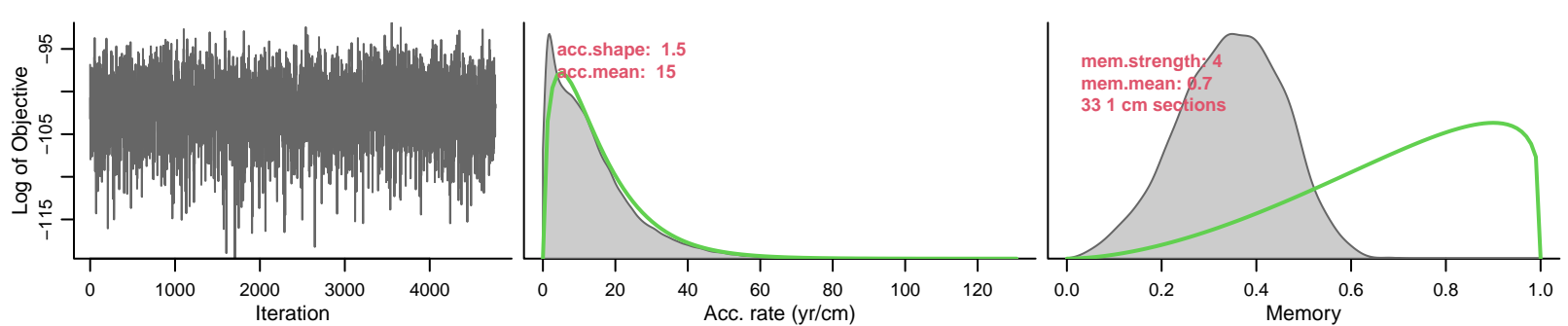


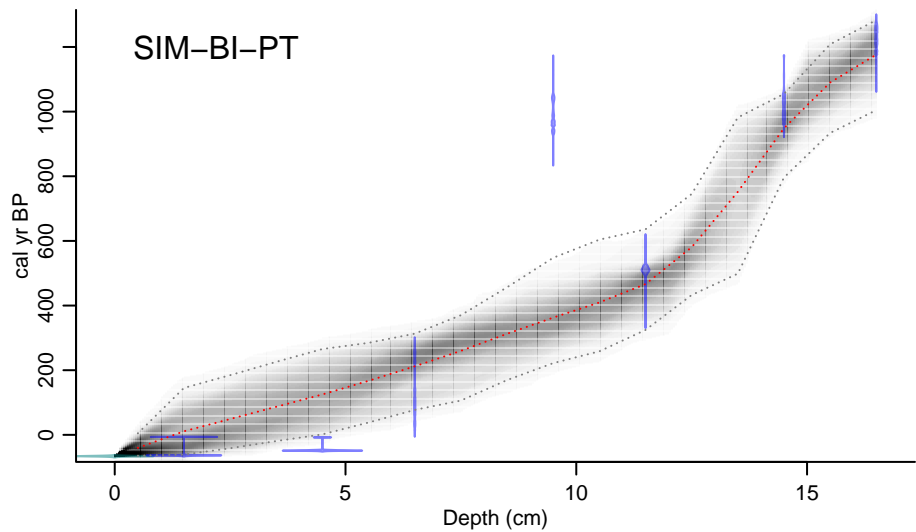
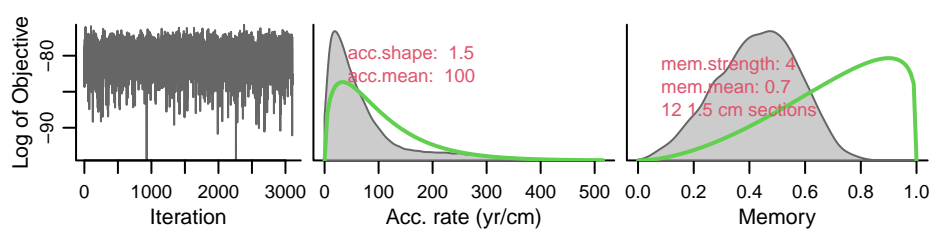




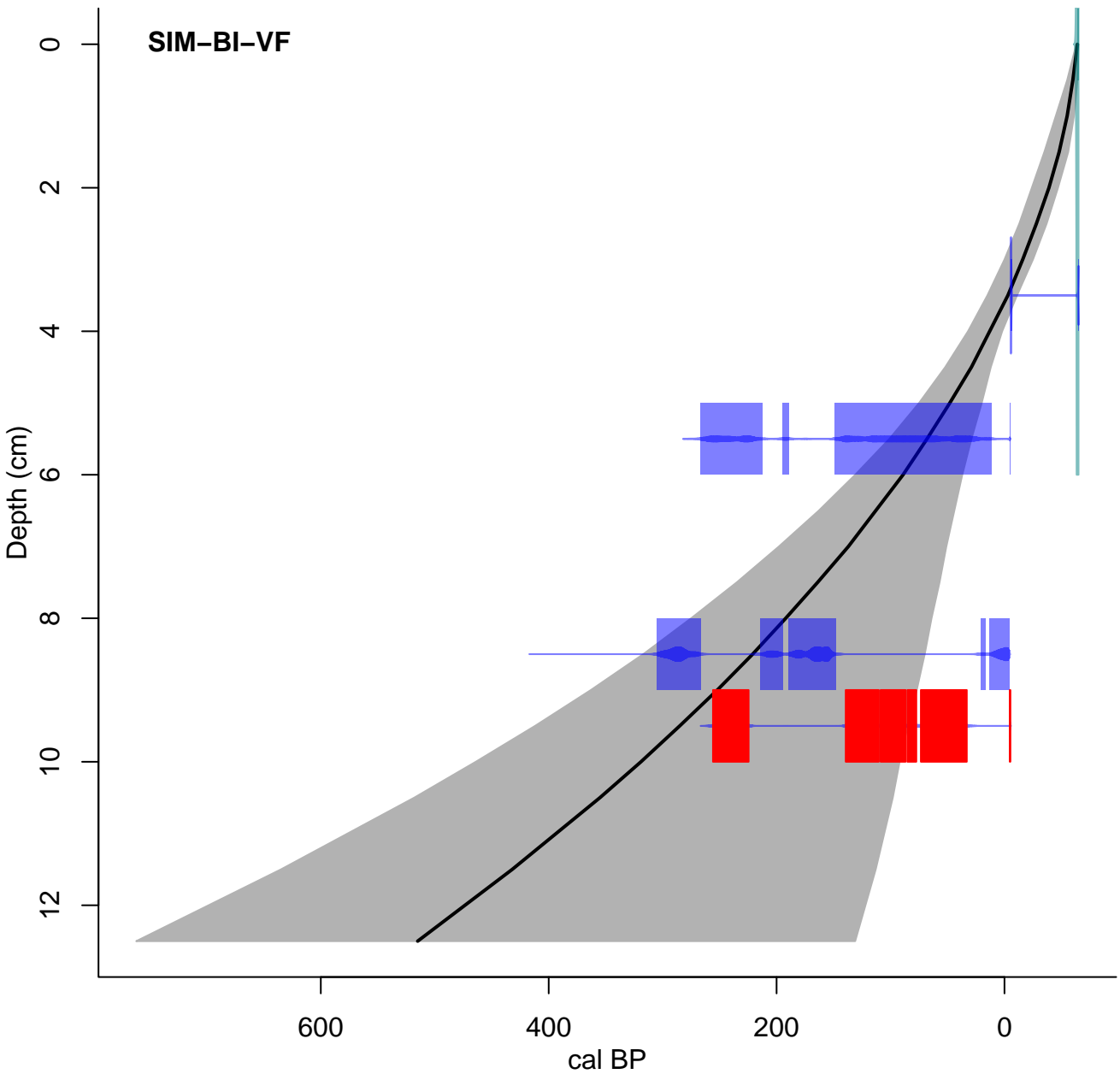




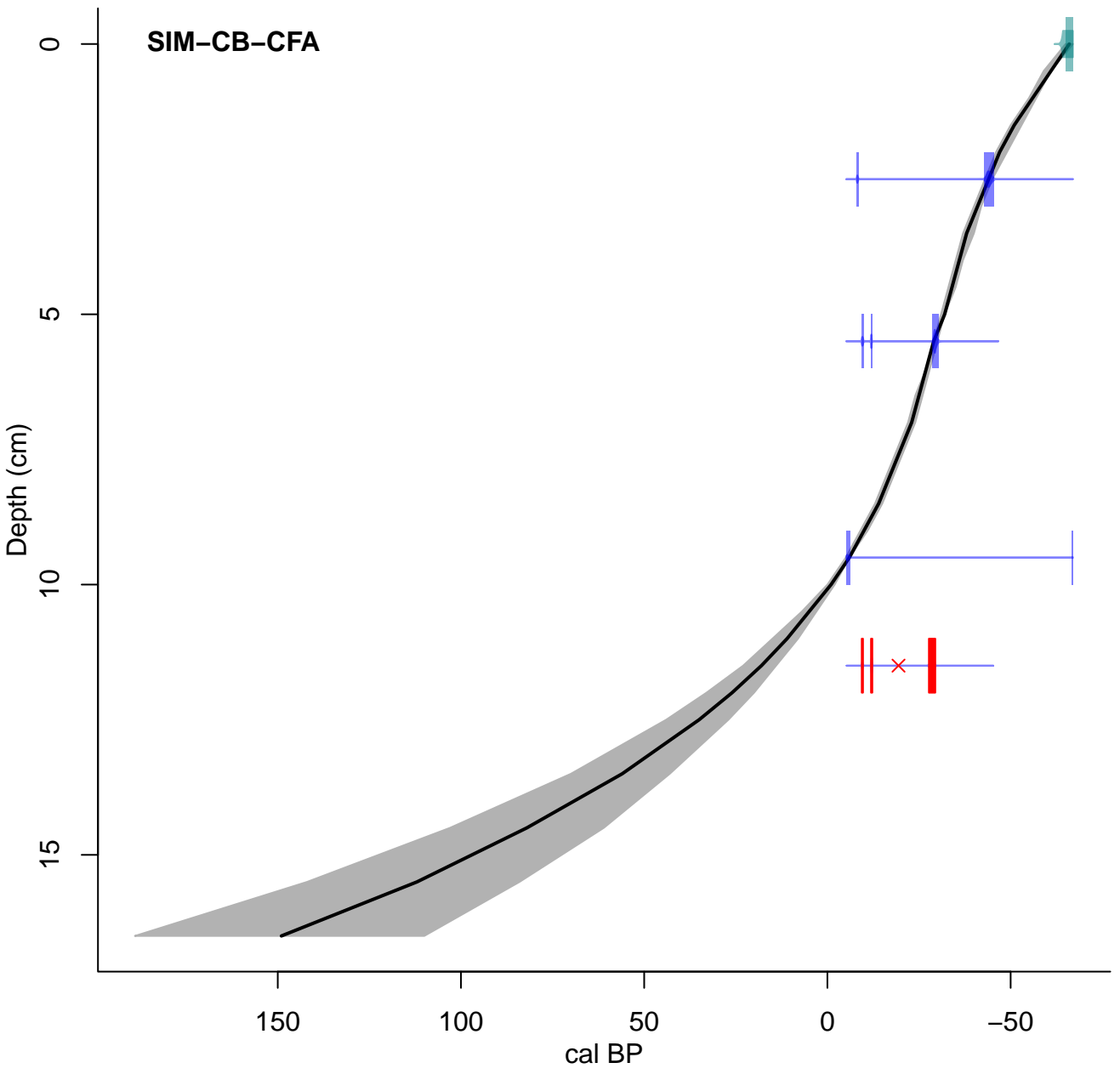


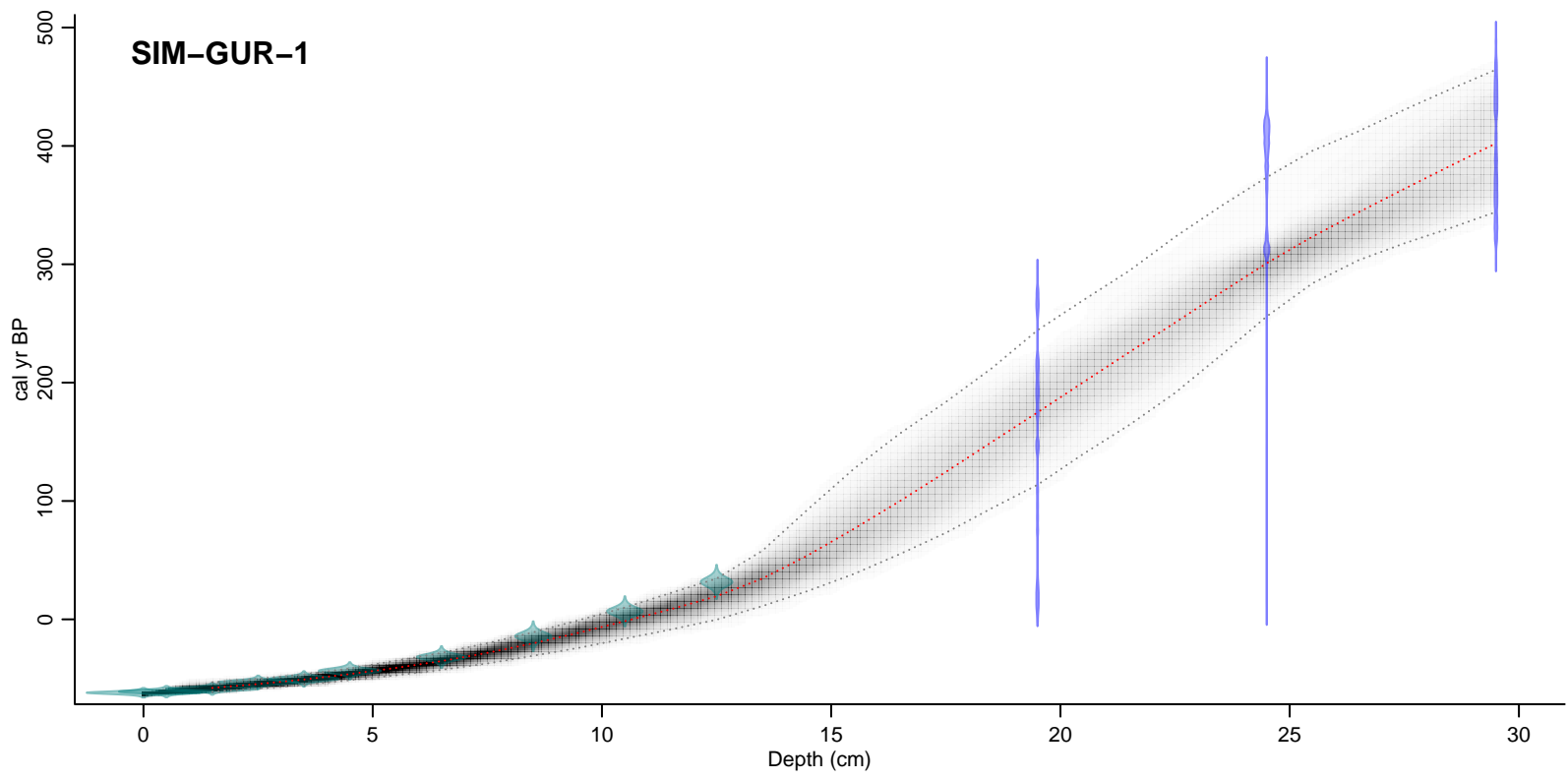
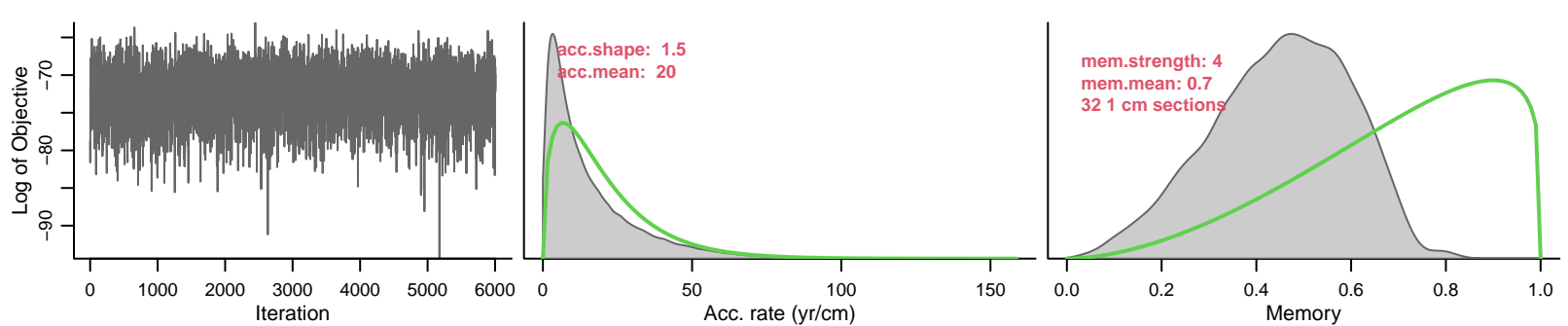


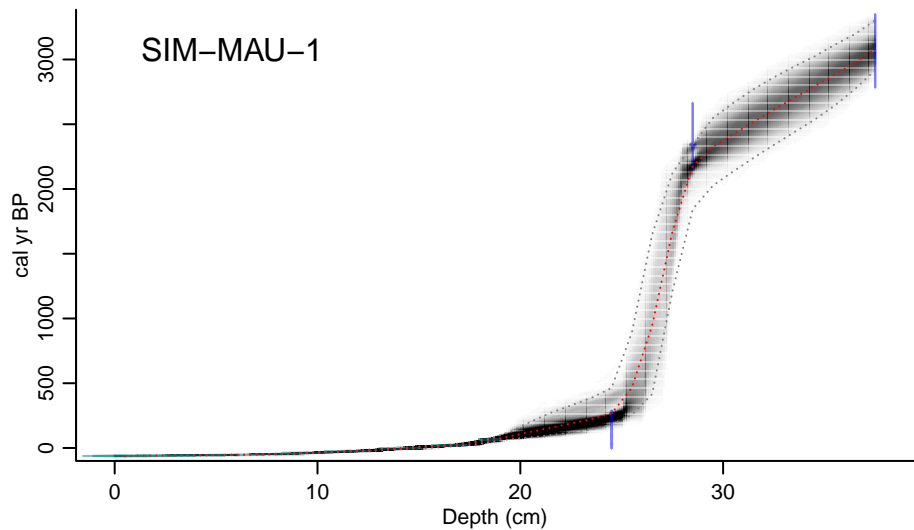
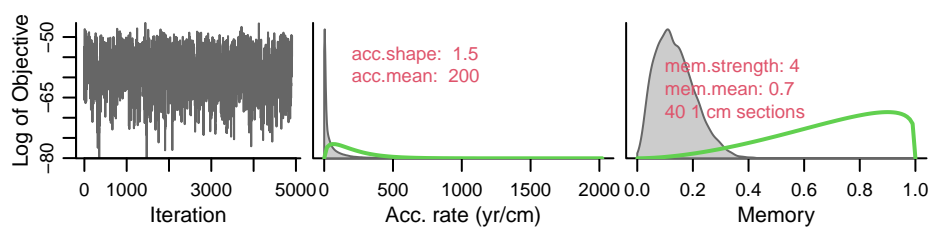
SIM-BI-VF

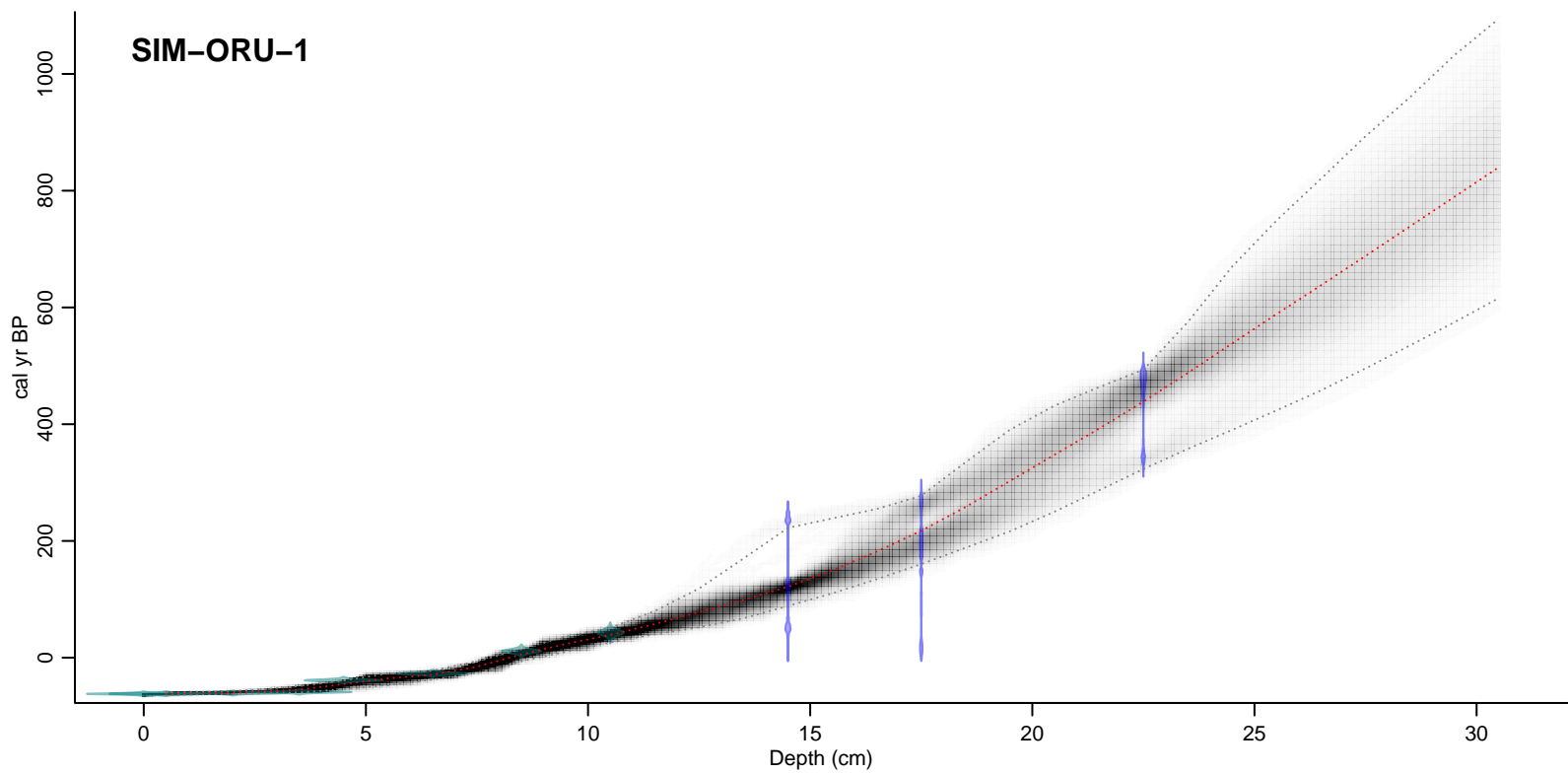
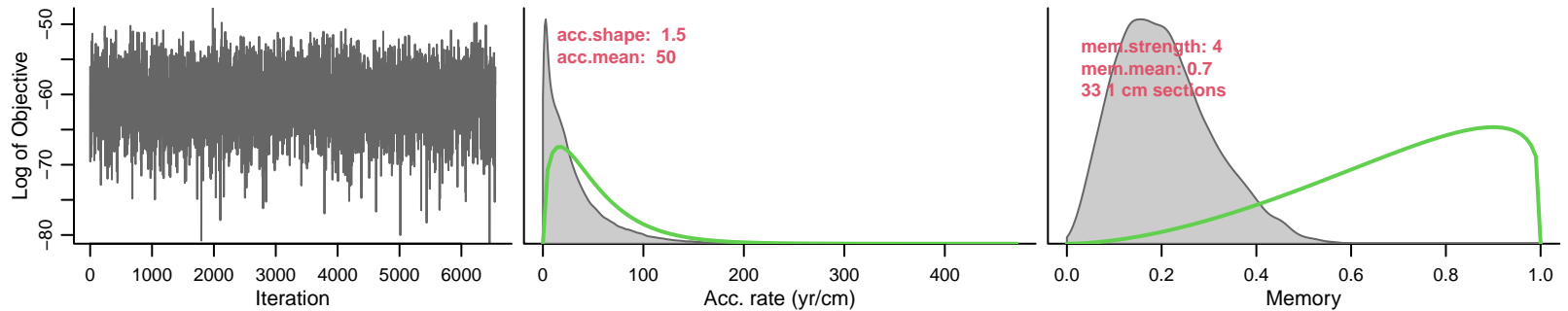


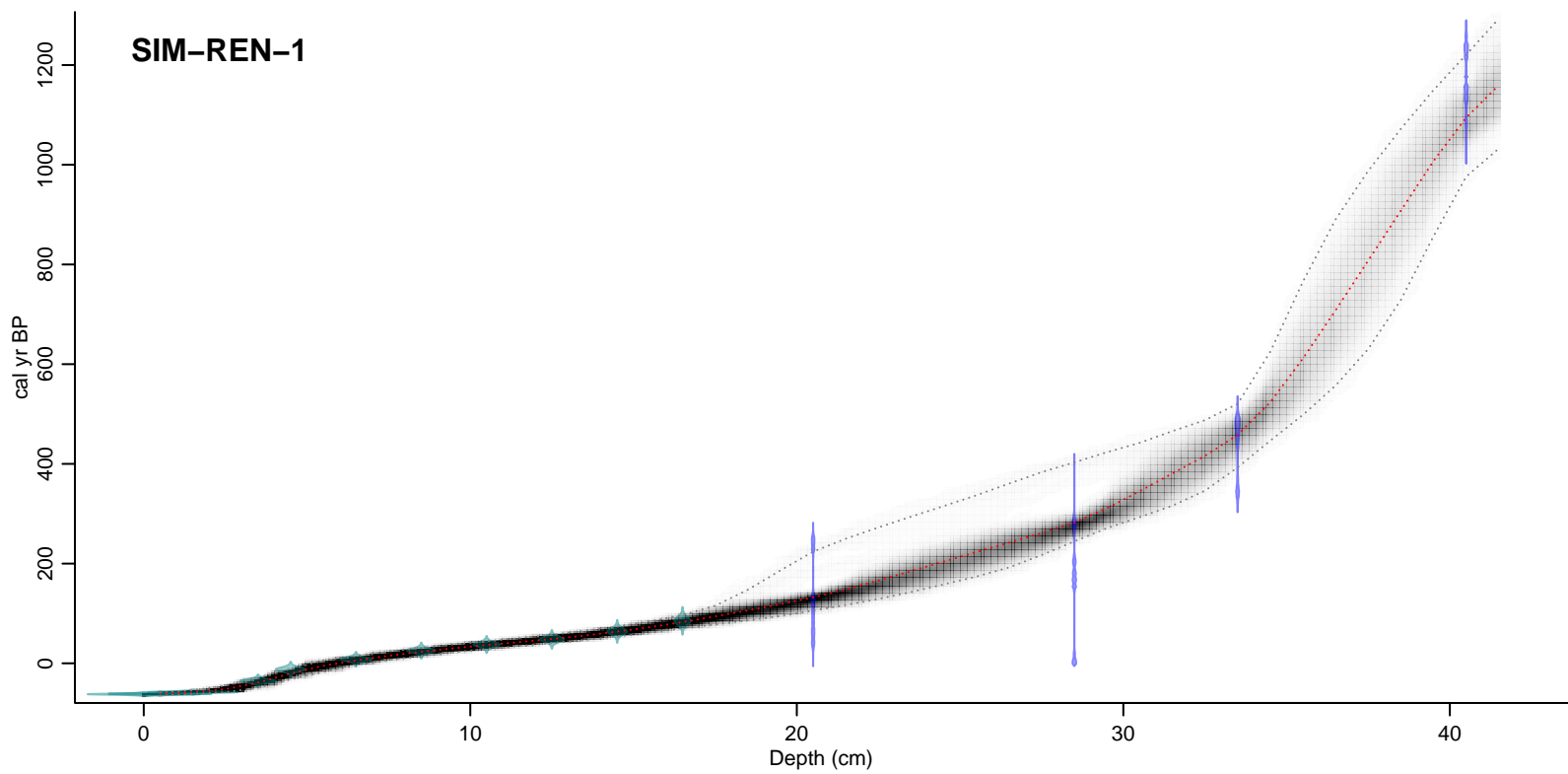
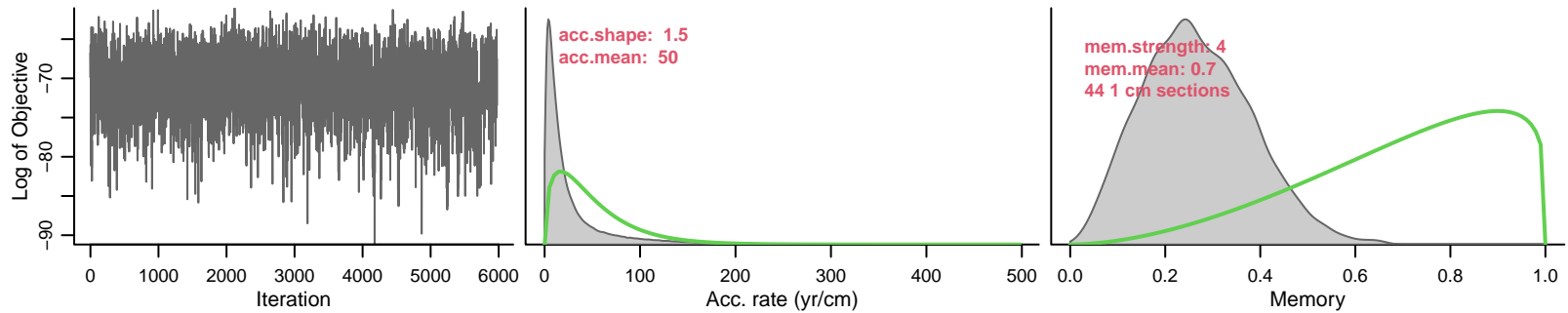
SIM-CB-CFA

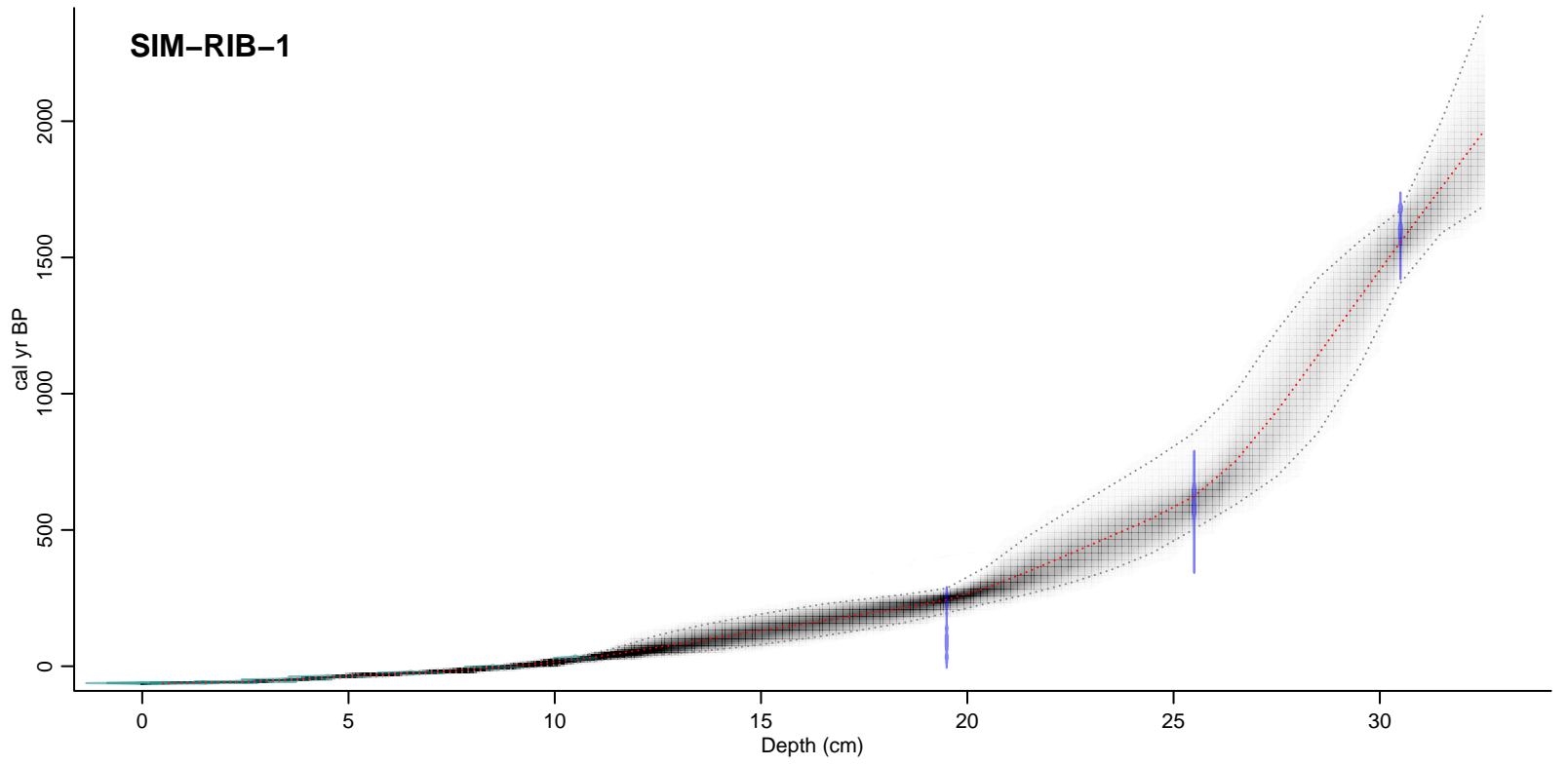
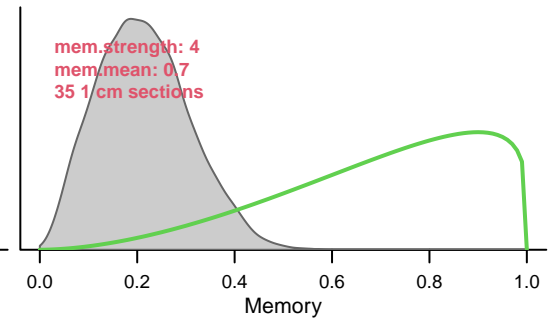
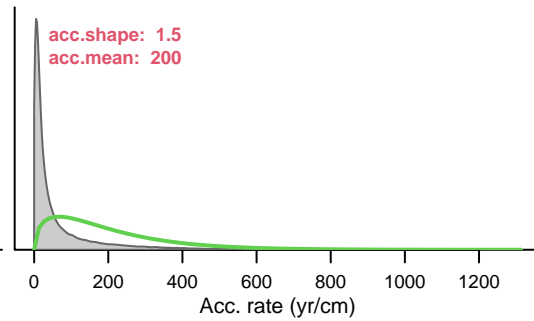
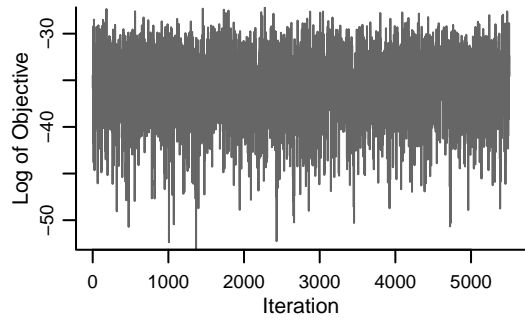


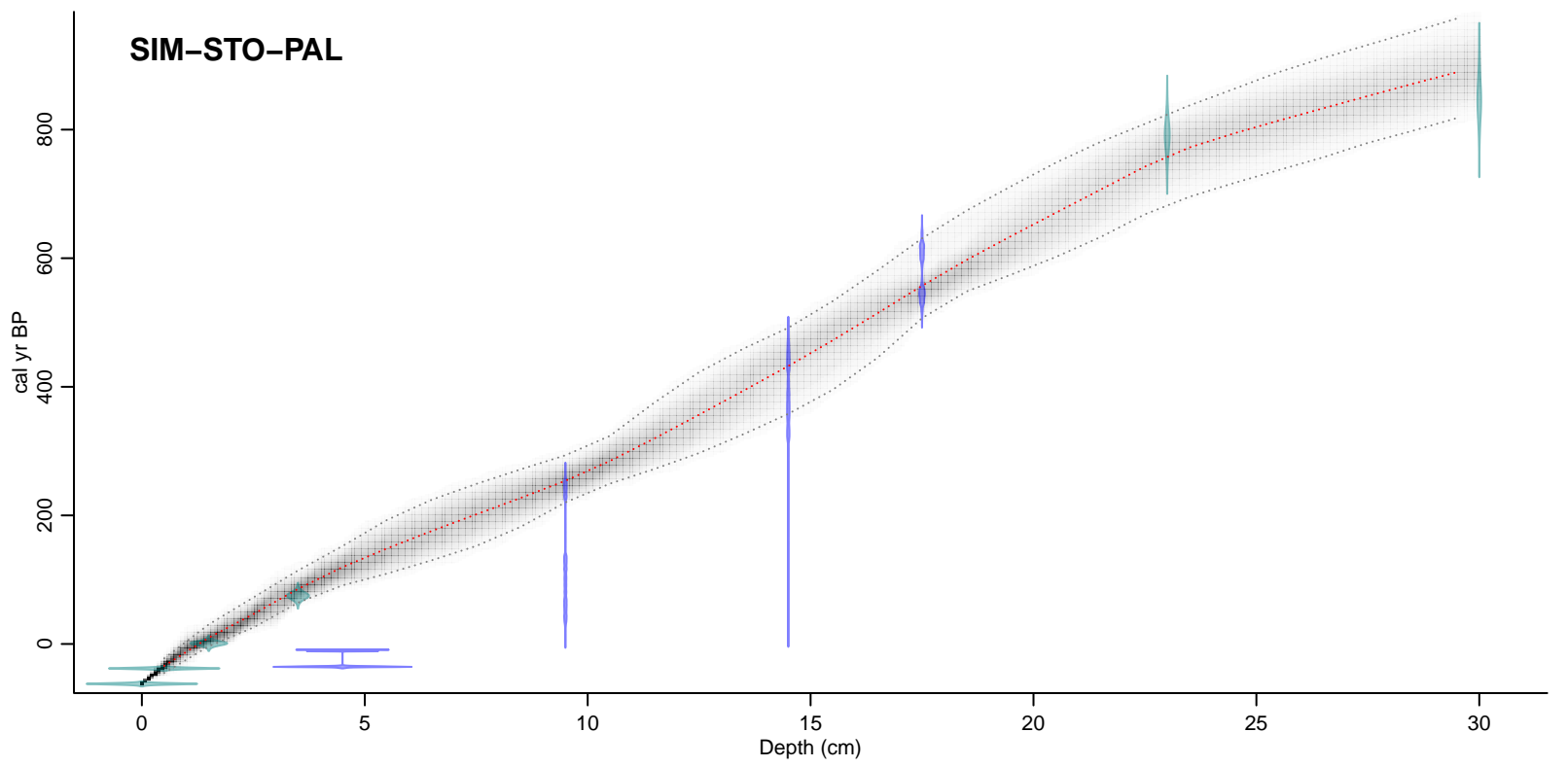
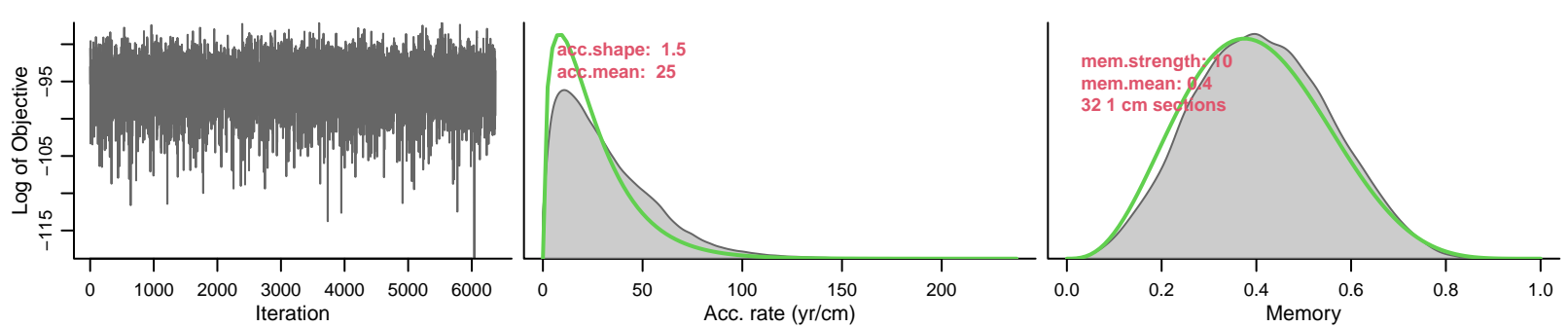


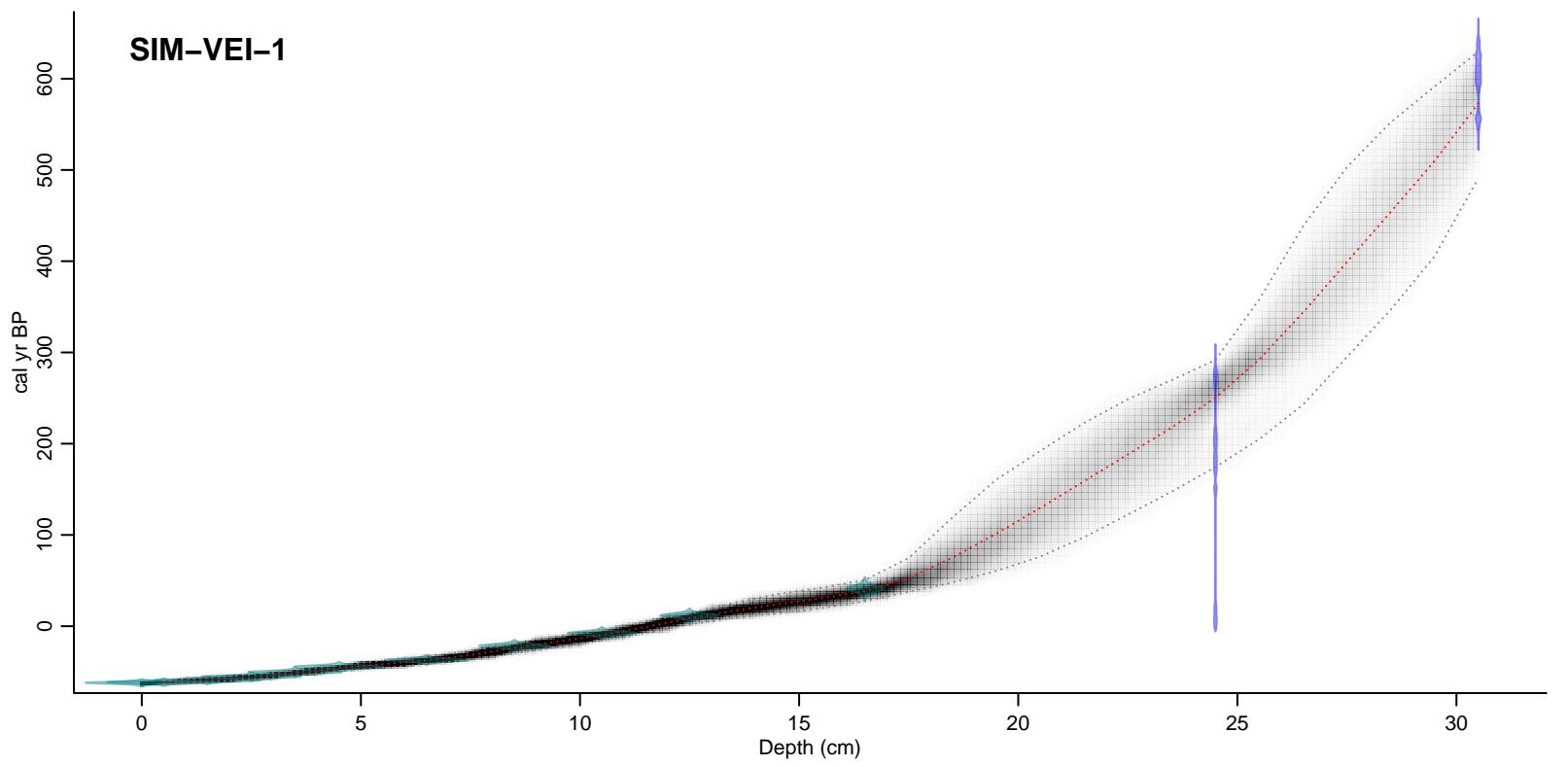
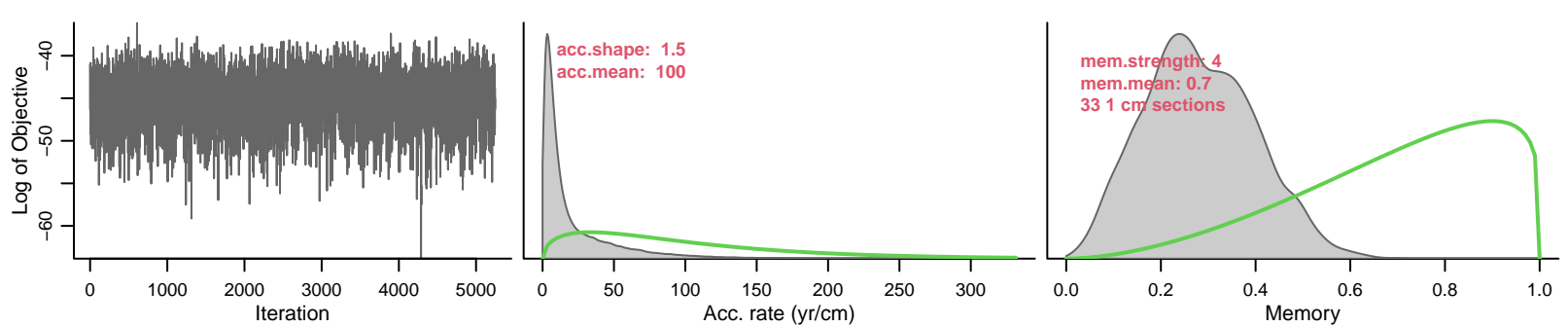


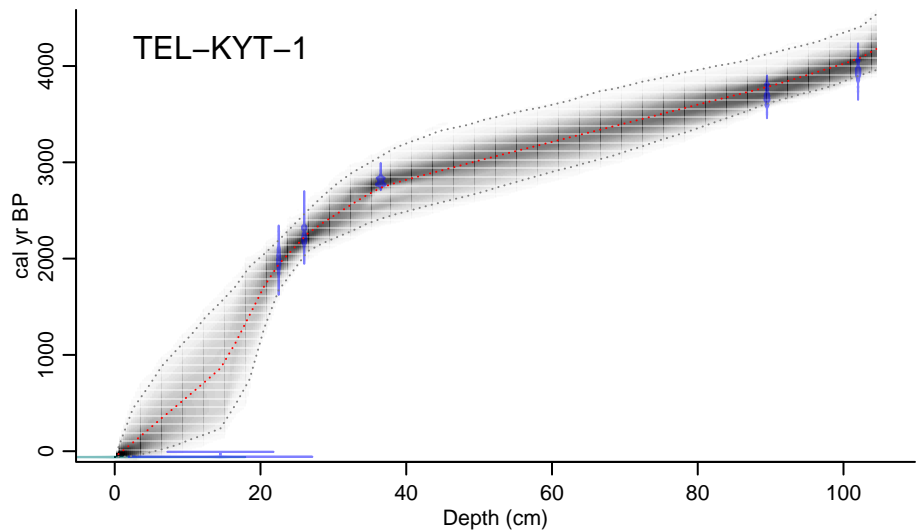
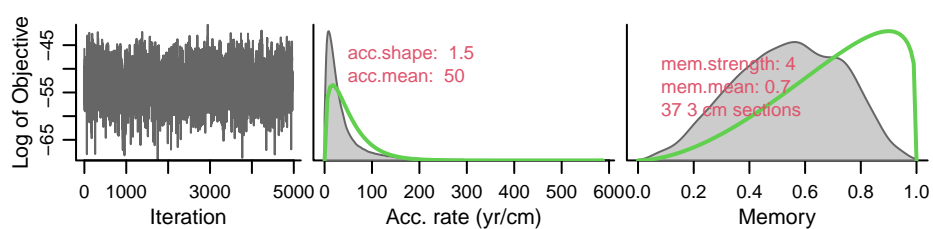




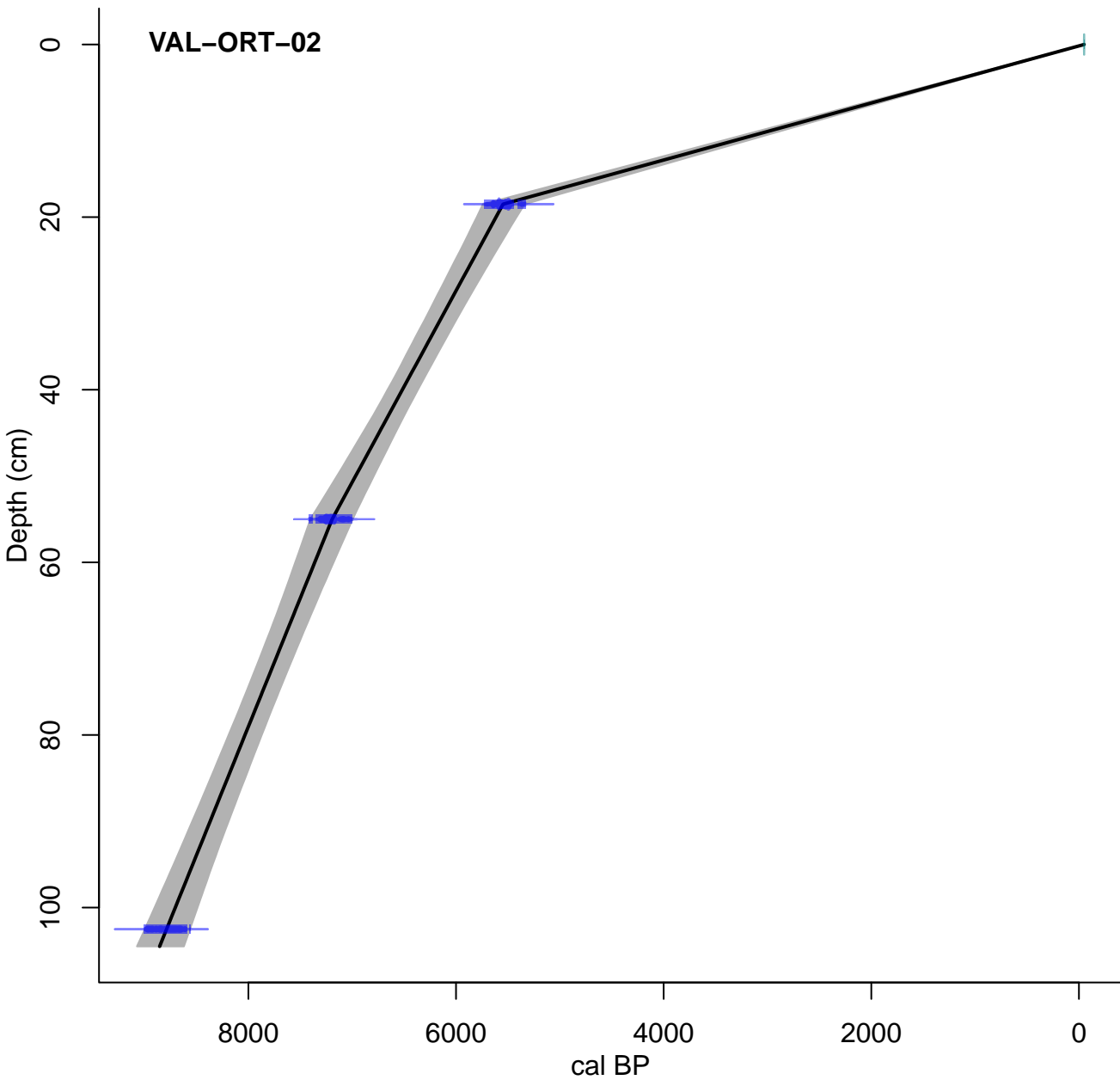


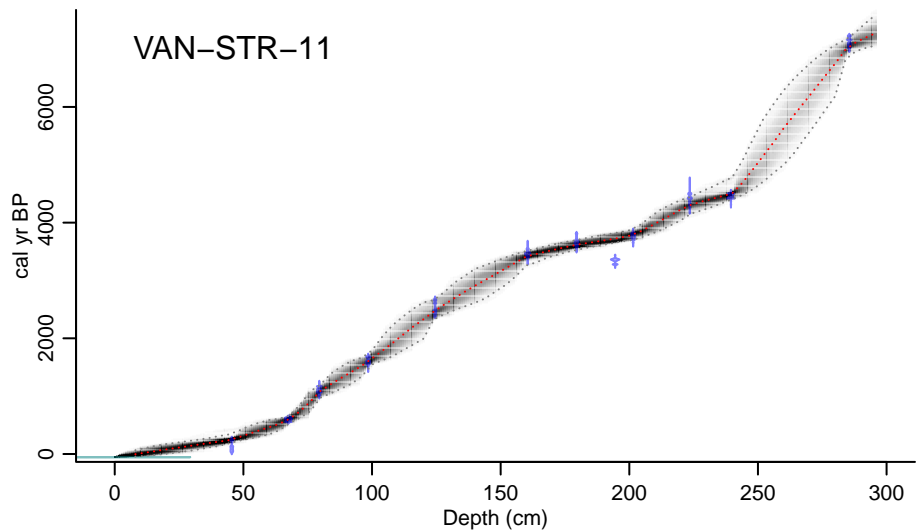
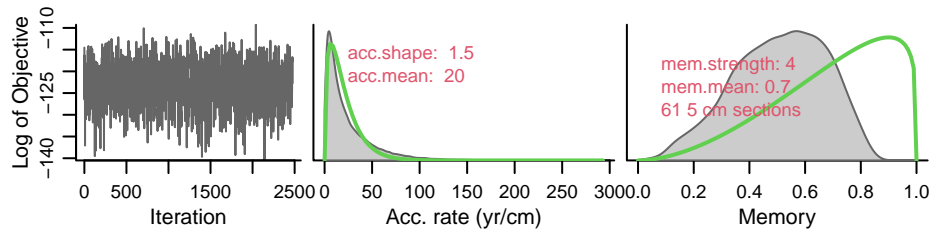




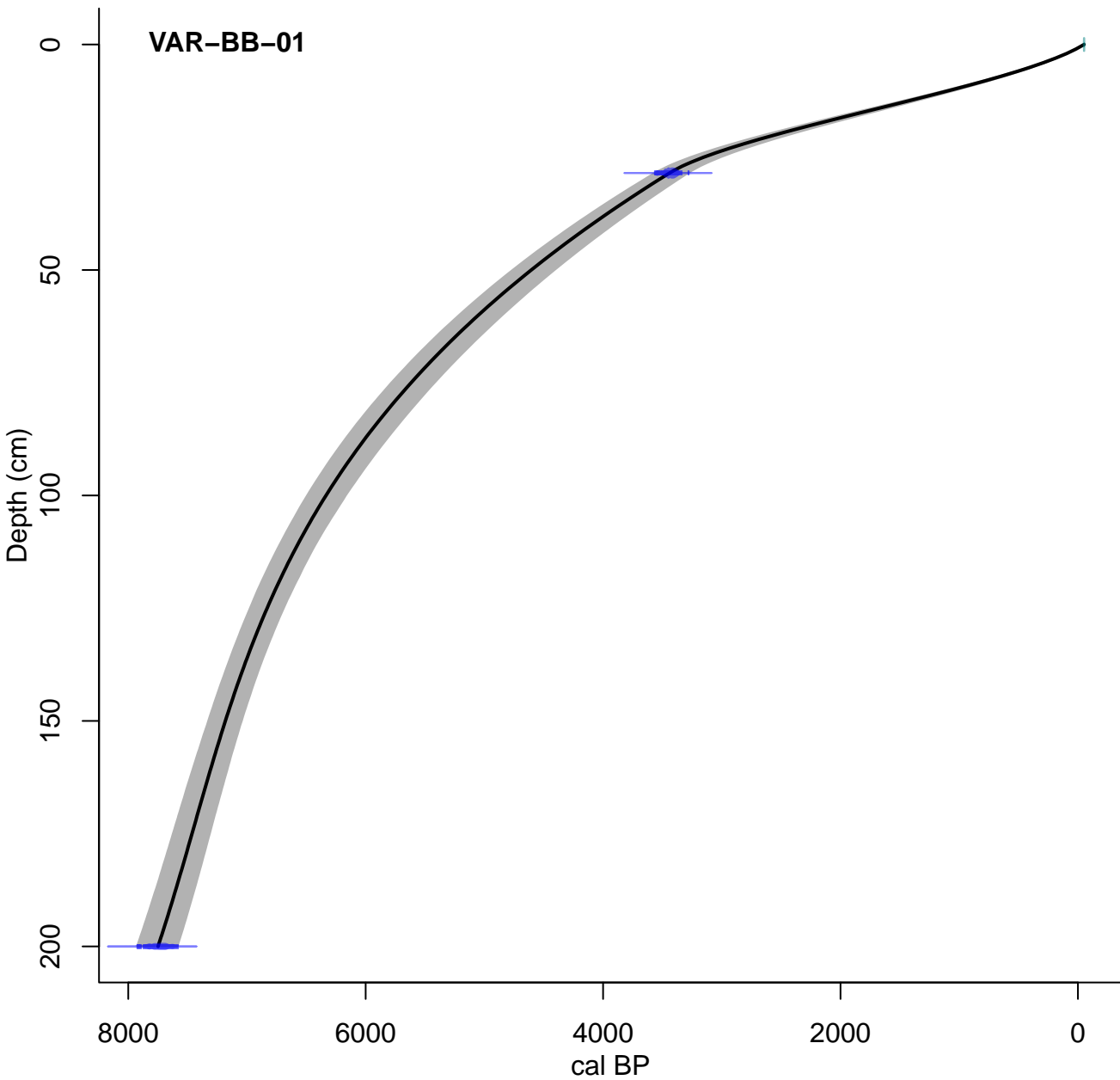


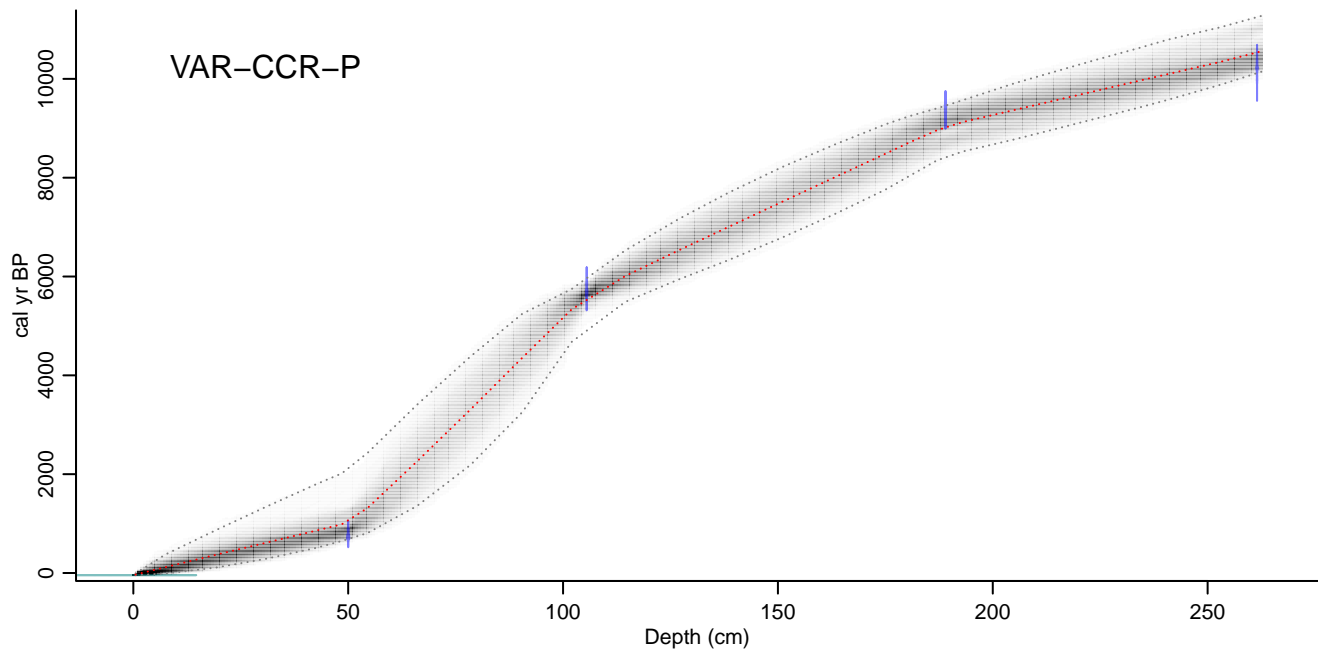
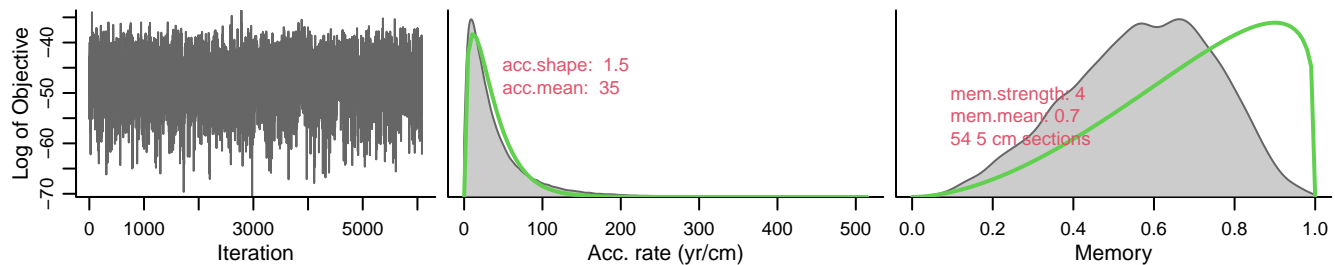
VAL-ORT-02

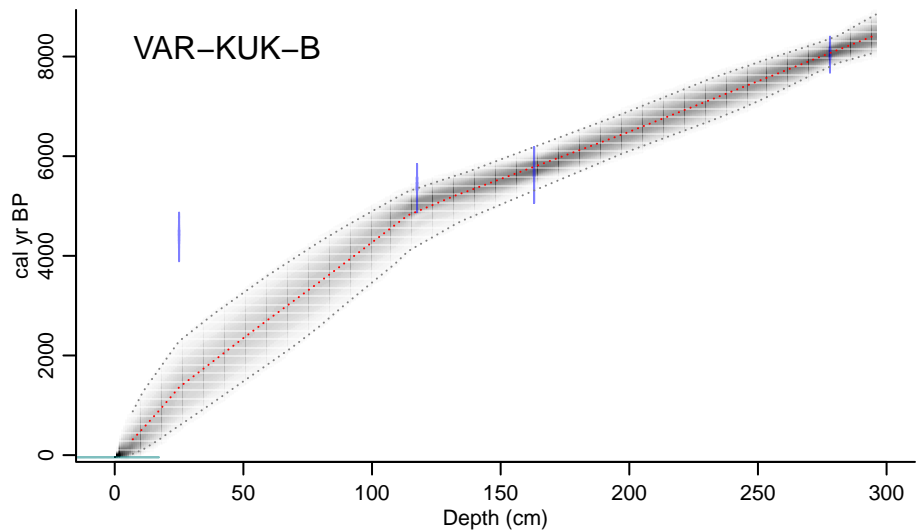
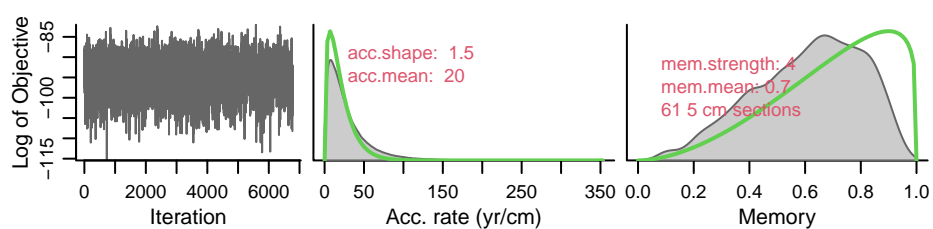




VAR-BB-01







VAR-TKP-01

